



Cite this: *Catal. Sci. Technol.*, 2021, 11, 2980

Received 2nd March 2021,  
Accepted 29th March 2021

DOI: 10.1039/d1cy00374g

rsc.li/catalysis

## Introduction

### Nickel catalysis in organic synthesis

The application of nickel catalysis in organic synthesis has been the subject of widespread investigation during the past ten to fifteen years, and is currently one of the most exciting frontiers in catalysis.<sup>1</sup> Many of the advances in nickel catalysis, such as the development of photoredox/cross-coupling reactions<sup>2,3</sup> and reductive cross-electrophile coupling<sup>4</sup> make use of the fact that nickel will readily access odd-numbered oxidation states.<sup>5</sup>

However, the rather different properties of nickel compared to palladium (for example) lead to additional mechanistic complexity that requires considerable effort and resource to understand. This review therefore focuses on both classic and newer studies that aim to understand reaction mechanisms and structure/reactivity relationships in the reactions of nickel(0) with organohalides.

### Reaction mechanisms

Before embarking on a detailed discussion of the literature, it is worthwhile to consider the mechanisms that might be in operation.<sup>6</sup> These can be divided into approximately five categories (Scheme 1), although the divisions between some mechanisms may be blurred, and there may be further nuance in the exact details. Nevertheless, we can broadly consider reactions to proceed *via* one of the following processes.

<sup>a</sup>WestCHEM Department of Pure & Applied Chemistry, University of Strathclyde, 295 Cathedral Street, Glasgow, G1 1XL, Scotland, UK.

E-mail: david.nelson@strath.ac.uk

<sup>b</sup>Chemical Development, Pharmaceutical Technology and Development, Operations, AstraZeneca, Macclesfield SK10 2NA, UK

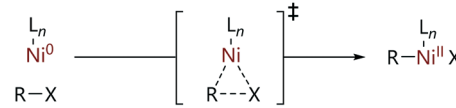
## Reactions of nickel(0) with organochlorides, organobromides, and organoiodides: mechanisms and structure/reactivity relationships

Megan E. Greaves, <sup>ab</sup> Elliot L. B. Johnson Humphrey<sup>a</sup> and David J. Nelson <sup>\*a</sup>

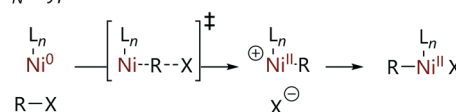
The reactions of nickel(0) complexes with organohalides have been reviewed. The review is divided according to the class of ligand that is present on nickel: phosphine, N-heterocyclic carbene, or bidentate nitrogen ligand. The preferred mechanism of reaction is often determined by a delicate balance of ligand and substrate structure, and relatively small changes can lead to large differences in behaviour. This will have an impact on the progress of catalytic reactions that use organohalide substrates, and may influence ligand selection and/or the scope and limitations of the reaction.

**Concerted oxidative addition.** Concerted oxidative addition, in which a carbon–halogen bond is cleaved in concert with the formation of a nickel–carbon and a nickel–halogen bond.

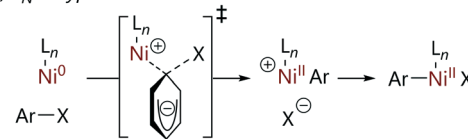
#### (a) Concerted Oxidative Addition



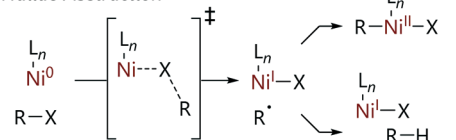
#### (b) S\_N2-type Oxidative Addition



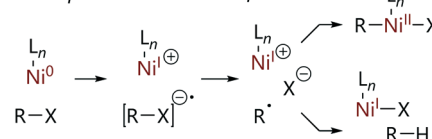
#### (c) S\_NAr-type Oxidative Addition



#### (d) Halide Abstraction



#### (e) Outer-Sphere Electron Transfer



**Scheme 1** Mechanisms for the reactions of nickel(0) complexes with organohalide substrates.



**S<sub>N</sub>2-Type oxidative addition.** In S<sub>N</sub>2-type oxidative addition (for alkyl halides) the nickel–carbon bond is formed as the carbon–halogen bond is cleaved. This will of course lead to the inversion of stereochemistry at the relevant centre.

**S<sub>N</sub>Ar-Type oxidative addition.** In S<sub>N</sub>Ar-type oxidative addition (for aryl halides) the nickel–carbon bond is formed as the carbon–halogen bond is cleaved. This might proceed *via* an intermediate Meisenheimer complex, as proposed for some reactions of palladium with aryl halides.<sup>7</sup>

**Halide abstraction.** In halide abstraction the carbon–halogen bond is cleaved during the formation of a nickel–halogen bond, forming a nickel(i) complex and an organic radical. This radical may recombine with the nickel(i) species, giving the formal oxidative addition product, or it may escape and undergo reactions such as hydrogen atom abstraction.

**Outer-sphere electron transfer.** Outer-sphere electron transfer is which the nickel(0) complex donates an electron into the carbon–halogen  $\sigma^*$ -orbital, leading to the formation of a cationic nickel species and a radical anion of the organohalide; the latter species is typically unstable and will eject a halide to form an organic radical. The resulting species might recombine to form the formal oxidative addition product, or might undergo other, separate reactions.

### Tools for mechanistic studies

The tools that can be used to study these reaction mechanisms are rather varied, and will depend on factors including the presence or absence of NMR active nuclides and whether the complexes of interest are paramagnetic or diamagnetic.

**Nickel(0) complexes.** As d<sup>10</sup> species that are typically linear two coordinate, trigonal planar, or tetrahedral, these are diamagnetic species that can be readily studied by NMR spectroscopy. The study of nickel(0)–phosphine complexes, and the monitoring of their reactions, can be conveniently carried out by <sup>31</sup>P NMR spectroscopy (provided the timescale is appropriate).

**Nickel(i) complexes.** These paramagnetic d<sup>9</sup> species are typically best studied by EPR spectroscopy,<sup>8</sup> although some dimeric complexes of this type are not amenable to study in this way due to interactions between the two nickel centres.<sup>9</sup> This technique allows the distinction to be made between complexes where there is a radical on the metal and those where the radical resides on the ligand(s); it also provides information on the geometry of the complex. Magnetic moment measurements using techniques such as Evans's method can be used to differentiate between nickel(i) and nickel(ii) complexes, as the expected values for  $\mu_{\text{eff}}$  are quite different. This method requires a sealed capillary with an internal standard (typically, but not necessarily, *tert*-butanol) placed in a solution with the analyte and *tert*-butanol. If the analyte is paramagnetic, the interaction with *tert*-butanol will shift the CH<sub>3</sub> signal on the <sup>1</sup>H NMR spectrum; the difference between  $\delta_{\text{H}}$  for the *tert*-butanol in the capillary (*i.e.* not in contact with the analyte) and  $\delta_{\text{H}}$  for the

*tert*-butanol in the same solution as the analyte can be used to calculate  $\mu_{\text{eff}}$ .

**Nickel(ii) complexes.** These d<sup>8</sup> species are paramagnetic if they are octahedral or tetrahedral, or diamagnetic if they are square planar. The first two geometries can be characterised using Evans's method, for example, while the study of these complexes by EPR is very challenging. Square planar nickel(ii) complexes are readily characterised and monitored by NMR spectroscopic methods.

Some tools that can be used to study and characterise these reaction pathways include:

**Kinetic studies.** These inevitably provide far more information than single time point analyses of reactions and can comprise a range of different types of analysis. The simple comparison of rate constants for species with different ligands can give useful information that can guide ligand selection and design, for example. The systematic variation of substrate concentrations allows the order in each substrate to be determined, either using the method of initial rates (provided that there is no initiation period) or the integral method (provided that data can be obtained to *ca.* 90% conversion). The change in rate constant as the temperature is varied allows the determination of the enthalpy and entropy of activation, with the latter quantity being especially informative when considering reaction mechanisms. Where the substrate(s) or ligands contain aryl groups, the systematic change of substitution pattern can be interpreted using a Hammett analysis.<sup>10</sup> Collecting sufficiently accurate, precise, robust, and reproducible kinetic data is often a challenge, but this can be achieved using time-resolved NMR, IR, or UV/visible spectroscopy, for example; alternatively, manual (or automated) sampling of reaction mixtures with appropriate quench and analysis steps might be an option. The exact approach will always depend on the precise system of interest.

**DFT studies.** We would argue that it is now possible for most non-specialists to conduct good quality DFT calculations of 'real' (or close to real) systems; sufficient computational horsepower is available within most institutions or may be available as part of national centres that accept applications from individual research groups. Even modern desktop computers with multicore processors are often sufficient to tackle smaller problems in organometallic reaction mechanisms. A full discussion of the opportunities and pitfalls is beyond the scope of this manuscript, but we would encourage new users of density functional theory to consult some useful introductory references<sup>11,12</sup> and consider the level of theory applied to systems that are similar to those of interest.<sup>13</sup> If we were to offer two pieces of advice, these would be: (i) ensure that a dispersion treatment is used, either through the use of a functional that includes it (*e.g.* M06,  $\omega$ B97X-D) or by the application of a dispersion correction (*e.g.* Grimme D3 or Grimme/Becke/Johnson D3(BJ)),<sup>14</sup> and (ii) be aware of the limitations of DFT in terms of system size, accuracy (a few kcal mol<sup>-1</sup>), and dealing with systems that have different spin states that are similar in energy.



## Scope of the review

This review considers the published literature to date on the topic of the reactions of organochloride, organobromide, and organoiodide compounds with nickel(0) complexes. The review will not consider the reactions of organofluorides, alcohol derivatives, trimethylammonium salts, diazonium salts, or any of the other alternative electrophiles for nickel-catalysed cross-coupling reactions.<sup>15,16</sup> The review is divided first by ligand class, and then by substrate type, with the narrative typically in approximately chronological order.

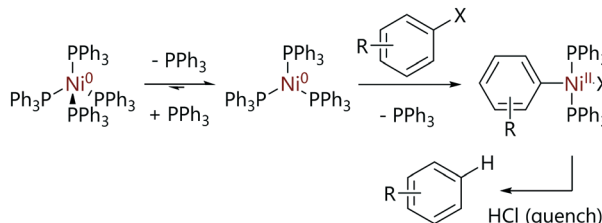
## Nickel(0) complexes with phosphorus ligands

### Reactions with aryl halides

The reactions of aryl halides with phosphine-ligated nickel(0) complexes have received attention as far back as the 1970s. Some aspects of this topic were recently reviewed by Pérez-Garcí and Moret.<sup>17</sup>

In 1970, Fahey reported the products of the reactions of  $[\text{Ni}(\eta^2\text{-C}_2\text{H}_4)(\text{PR}_3)_2]$  ( $\text{R} = \text{Et}$  or  $\text{Ph}$ ) with bromopentafluorobenzene, chlorotrifluoroethylene, 1,2,4-trichlorobenzene, 1,2-dichlorobenzene, and 1-bromo-2-chlorobenzene;<sup>18</sup> these were obtained in 6–19% yield and formulated as the *trans*- $[\text{Ni}(\text{X})(\text{R}')(\text{PR}_3)_2]$  complexes based on infrared analysis which revealed a strong band at *ca.* 420  $\text{cm}^{-1}$  that is proposed to correspond to an asymmetric Ni–P stretching vibration. The regioselectivity of the oxidative addition reaction of 1,2,4-trichlorobenzene was confirmed by quenching the resulting complex with acid; this formed a mixture of 1,2-dichlorobenzene (7%), 1,3-dichlorobenzene (6%), and 1,4-dichlorobenzene (87%). The selectivity for the 2-position was taken as possible evidence of an  $\text{S}_{\text{N}}\text{Ar}$ -type oxidative addition transition state by comparison of the regiochemistry of the corresponding reaction between 1,2,4-trichlorobenzene and methoxide. However, the relative rate of C–Br *versus* C–Cl activation (as determined from the outcomes of the reactions of 1-bromo-2-chlorobenzene) was *ca.* 0.003, much lower than would be expected for an  $\text{S}_{\text{N}}\text{Ar}$  reaction (*ca.* 0.1–1) but similar to that observed for the  $\text{S}_{\text{N}}2$  reactions of alkyl halides and cobaloximes (*ca.* 0.0015–0.023).

In 1975, Foa and Cassar investigated the rates of oxidative addition of  $[\text{Ni}(\text{PPh}_3)_4]$  with various *para*-substituted aryl halides (Scheme 2); the majority of kinetic experiments were conducted with aryl chlorides.<sup>19</sup>  $[\text{Ni}(\text{PPh}_3)_3]$  forms



Scheme 2 Reactions studied by Foa and Cassar.<sup>19</sup>

spontaneously when solid  $[\text{Ni}(\text{PPh}_3)_4]$  is dissolved in solution and so this is the active species.<sup>20</sup> The oxidative addition reactions were found to be first order in aryl halide and inhibited by triphenylphosphine when excess ligand was added to kinetic experiments.

Relative rates of oxidative addition for differently-substituted aryl halides were measured using competition reactions; in these experiments, equimolar quantities of two aryl halides were mixed and  $[\text{Ni}(\text{PPh}_3)_4]$  (10 mol%) was added. The reaction mixture was quenched with a saturated  $\text{HCl}/\text{Et}_2\text{O}$  solution and the proportions of the hydrocarbons formed were quantitatively determined by gas chromatography. These data were used to determine relative rates of reaction, which were plotted using a Hammett treatment (Fig. 1). A good correlation was observed for electron-withdrawing substituents, and a large value of  $\rho$  was obtained ( $>8$ ). A dramatic change of gradient to *ca.* 0.25 was observed for substituents where  $\sigma < 0.23$ . The relative rates of reaction for aryl chlorides and aryl bromides with the same aryl substitution pattern were often very different depending on the aryl fragment; for haloarenes with electron withdrawing substituents the reaction was approximately one hundred times faster with an aryl bromide compared to a chloride, but this difference was decreased to two to three times when an electron donating substituent was present. The authors proposed that the evidence suggested a concerted three-centre oxidative addition process, although the sudden change in slope of the Hammett plot could be indicative of different reaction mechanisms depending on how electron-rich the substrate is.

In what is widely regarded as the seminal study of oxidative addition to nickel(0), the mechanism of the reaction of  $[\text{Ni}(\text{PEt}_3)_4]$  with aryl halides was extensively probed in 1979

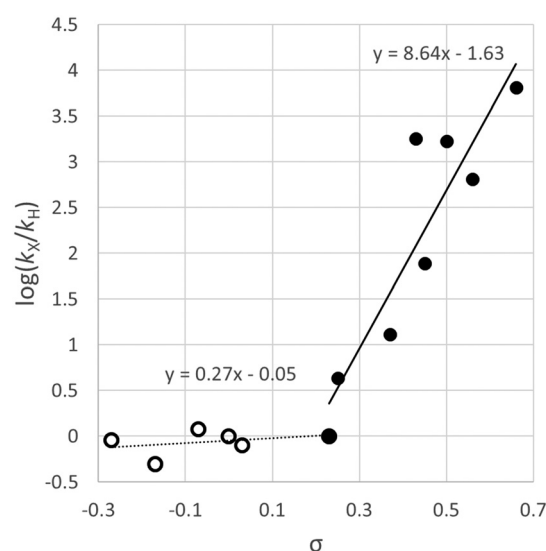
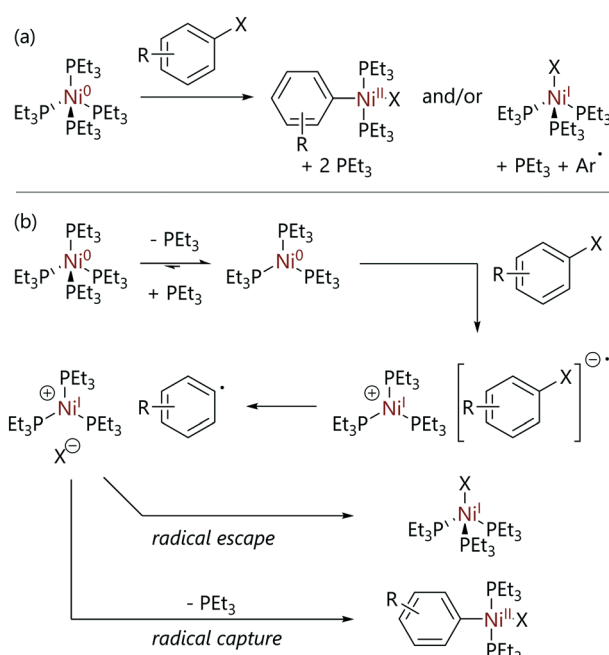


Fig. 1 Hammett plot constructed from data reported by Foa and Cassar for the reactions of  $[\text{Ni}(\text{PPh}_3)_4]$  with substituted aryl chlorides indicating a relatively flat regime ( $\rho = 0.27$ ) for electron-rich substrates and a steep slope ( $\rho = 8.6$ ) for electron-poor substrates.<sup>19</sup>



by Tsou and Kochi.<sup>21</sup> The reactions of  $[\text{Ni}(\text{PEt}_3)_4]$  with various *para*-substituted aryl halides yielded both  $[\text{Ni}(\text{Ar})\text{X}(\text{PEt}_3)_2]$  and  $[\text{NiX}(\text{PEt}_3)_3]$  complexes as products, in ratios that depended on the structure of the aryl halide and the reaction solvent (Scheme 3(a)). Notably, a (slow) further reaction of  $[\text{NiX}(\text{PEt}_3)_3]$  with another molecule of aryl halide was observed, to form  $[\text{NiX}_2(\text{PEt}_3)_2]$  plus an aryl radical that likely abstracts hydrogen from the solvent (Scheme 1). The formation of  $[\text{Ni}(\text{Ar})\text{X}(\text{PEt}_3)_2]$  was monitored *via* IR spectroscopy and the formation of  $[\text{NiX}(\text{PEt}_3)_3]$  was monitored *via* EPR spectroscopy. The formation of  $[\text{NiX}(\text{PEt}_3)_3]$  *via* comproportionation between  $[\text{Ni}(\text{PEt}_3)_4]$  and  $[\text{Ni}(\text{Ar})\text{X}(\text{PEt}_3)_2]$  was ruled out using control experiments.

It was found that a number of factors affect the ratio of  $[\text{Ni}(\text{Ar})\text{X}(\text{PEt}_3)_2]$  to  $[\text{NiX}(\text{PEt}_3)_3]$  formed during each reaction, including: the identity of the halide; the substitution pattern of the aryl substituent; the reaction solvent; and the phosphine ligand. The quantity of the paramagnetic species  $[\text{NiX}(\text{PEt}_3)_3]$  was a function of the identity of  $\text{X}$  ( $\text{I} \gg \text{Br} > \text{Cl}$ ); an increase in the amount of nickel(i) formed was also observed in more polar solvents (hexane  $<$  toluene  $<$  THF). There was no correlation between the product ratio and the identity of the *para*-substituents on the aryl substrates used, although positively charged substituents increased the amount of  $[\text{NiX}(\text{PEt}_3)_3]$ , whilst negatively charged substituents decreased nickel(i) formation. Although the identity of the ligand attached to nickel would influence the reactivity of nickel(0) initially, the speciation of the nickel(0) species (*i.e.*  $[\text{Ni}(\text{PEt}_3)_4]$ ,  $[\text{Ni}(\text{PEt}_3)_3]$ , or  $[\text{Ni}(\text{PEt}_3)_2]$ ) had no effect on product distribution but the reaction rate was decreased if additional triethylphosphine was added.



**Scheme 3** (a) The outcomes of the reactions of  $[\text{Ni}(\text{PEt}_3)_4]$  with aryl halides ( $\text{X} = \text{Cl}, \text{Br}, \text{or I}$ ) to form  $[\text{Ni}(\text{Ar})\text{X}(\text{PEt}_3)_2]$  and/or  $[\text{NiX}(\text{PEt}_3)_3]$ .<sup>21</sup> (b) The reaction mechanism proposed initially.

In solution,  $[\text{Ni}(\text{PEt}_3)_4]$  readily dissociates triethylphosphine to form  $[\text{Ni}(\text{PEt}_3)_3]$  ( $K_{\text{eq}} = 1.2 \times 10^{-2} \text{ mol L}^{-1}$  in benzene at  $25^{\circ}\text{C}$ ).<sup>20</sup> After this pre-equilibrium is established, the proposed mechanism for this reaction involves the collapse of a charged ion pair in the rate-limiting transition state (Scheme 3(b)). This proposal was supported by previous studies that showed that single-electron transfer from nickel to an electron-acceptor was feasible;  $[\text{Ni}(\text{PEt}_3)_4]$  rapidly reduced tetracyanoethylene (amongst other electron-acceptors) to generate radical anions that were detected by EPR spectroscopy.<sup>22</sup> The cage collapse of this charged ion pair and the ratios of products formed ( $[\text{Ni}(\text{Ar})\text{X}(\text{PEt}_3)_2]$  or  $[\text{NiX}(\text{PEt}_3)_3]$ ) was proposed to depend on the stability and lifetime of the ion pair, which in turn depends on reaction variables such as the halide identity, the aryl *para*-substituent, the reaction solvent, and the ligands attached to nickel.

To support this mechanism, cyclic voltammetry was used to study the reactions of  $[\text{Ni}(\text{PEt}_3)_3]$  with various *para*-substituted aryl chlorides, bromides and iodides. A Hammett plot with a positive slope, indicating a build-up of negative charge in the transition state, was consistent with the formation of a radical anion. A linear relationship was found between the rate constants for oxidative addition of  $[\text{Ni}(\text{PEt}_3)_3]$  to aryl halides and the reduction of aryl halides, suggesting a similar transition state.

Funes-Ardoiz *et al.* later explored this system using DFT calculations of a  $[\text{Ni}(\text{PMe}_3)_4]$  model system, with some calculations on the corresponding  $\text{PMe}_2\text{Ph}$ ,  $\text{PMePh}_2$ , and  $\text{PPh}_3$  systems. Chloro-, bromo-, and iodobenzene were used as model substrates. This study concluded that the nickel-containing products –  $[\text{Ni}(\text{Ar})\text{X}(\text{PMe}_3)_2]$  and  $[\text{NiX}(\text{PMe}_3)_3]$  – arise from two competing pathways: an  $\text{S}_{\text{N}}\text{Ar}$ -type oxidative addition, without an Meisenheimer intermediate, to  $[\text{Ni}(\text{PMe}_3)_3]$  leads to the formation of  $[\text{Ni}(\text{Ar})\text{X}(\text{PMe}_3)_2]$  and a halide abstraction mechanism to the formation of  $[\text{NiX}(\text{PMe}_3)_3]$  (Fig. 2).<sup>23</sup>

Both mechanisms were shown to proceed through  $[\text{Ni}(\text{PMe}_3)_3]$  as opposed to  $[\text{Ni}(\text{PMe}_3)_4]$ ,  $[\text{Ni}(\text{PMe}_3)_2]$ , or  $[\text{Ni}(\text{PMe}_3)]$ ; the latter two species were found to be rather high in energy. The identity of halide that was used had little influence on the energetics of the  $\text{S}_{\text{N}}\text{Ar}$  mechanism; however, a broad range of energies were obtained for the halide abstraction pathway for aryl chlorides, bromide and iodides, consistent with the rather different C–Cl, C–Br, and C–I bond strengths. The reaction selectivity was found to depend on the relative energies of the transition states of the  $\text{S}_{\text{N}}\text{Ar}$  type mechanism and the halide abstraction mechanism. The  $\text{S}_{\text{N}}\text{Ar}$  reaction was favoured for chlorobenzene, similar in energy to halide abstraction for bromobenzene, and much higher in energy than halide abstraction for iodobenzene. Microkinetic modelling using DFT-derived energies allowed the experimentally-observed ratio of products to be reproduced to a reasonable degree of accuracy.

Experimental evidence for these two competing mechanisms was provided by Manzoor *et al.* who studied the



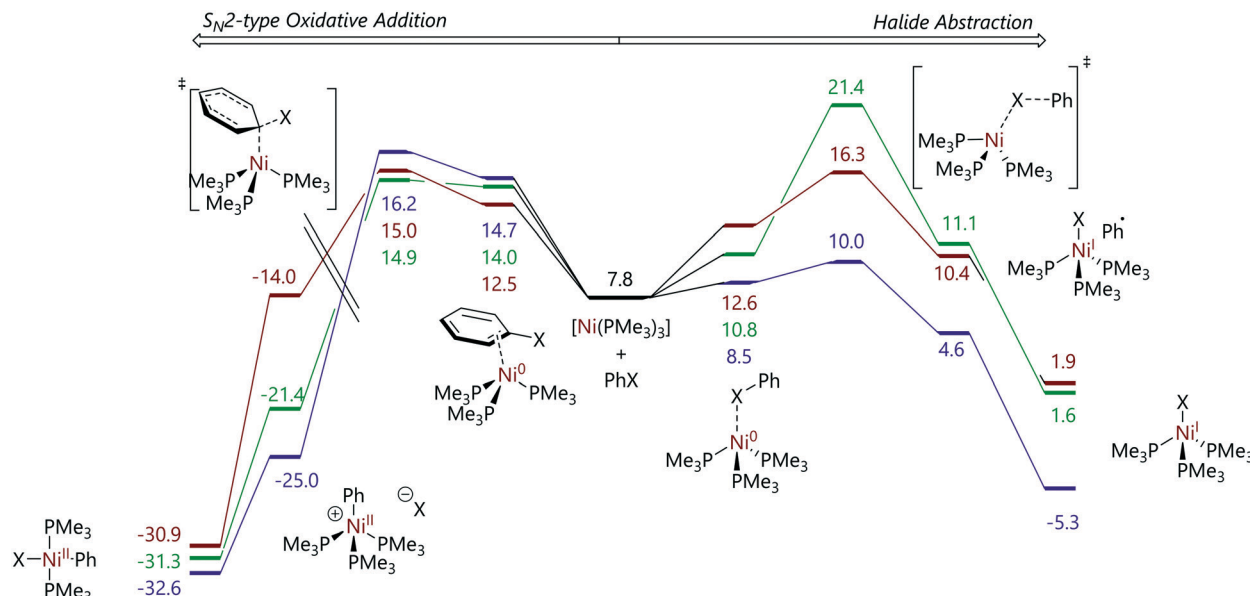


**Fig. 2** Profiles for the reactions of chloro- (green), bromo- (brown), and iodobenzene (purple) with  $[Ni(PMe_3)_3]$  from DFT calculations. Energies are free energies in kcal mol<sup>-1</sup> and are quoted relative to  $[Ni(PMe_3)_4]$ . Left:  $S_NAr$ -type oxidative addition for which the barriers are relatively insensitive to halide identity. Right: Halide abstraction for which the barriers are strongly dependent on halide identity.<sup>23</sup> Note that the energy scale on the left-hand side is discontinuous.

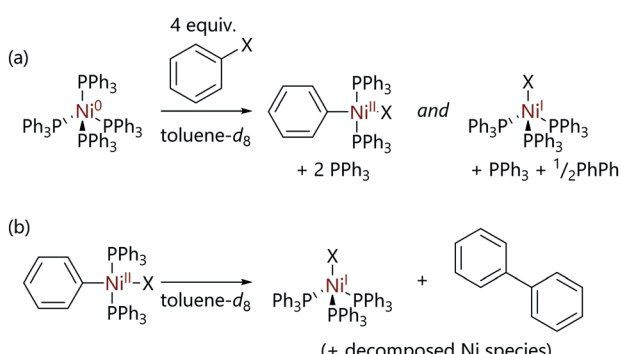
reactions of  $[Ni(PPh_3)_4]$  with halobenzene substrates using NMR spectroscopy.<sup>24</sup> Typical stoichiometric experiments involved exposing  $[Ni(PPh_3)_4]$  to the substrate at low temperatures in the NMR spectrometer, followed by gradually increasing the temperature in stages and observing the sample composition. The major product of the reactions of  $[Ni(PPh_3)_4]$  with chlorobenzene or bromobenzene was found to be (diamagnetic) *trans*- $[Ni(Ph)X(PPh_3)_2]$ , which was characterised by <sup>1</sup>H NMR spectroscopy (Scheme 4(a)). However, when iodobenzene was used as the substrate the major product was paramagnetic  $[NiI(PPh_3)_3]$ , consistent with previous observations by Kochi whilst studying reactions of  $[Ni(PEt_3)_4]$ .<sup>21</sup>

After the oxidative addition of chlorobenzene to nickel(0) was complete, the slow decomposition of *trans*- $[Ni(Ph)(X)(PPh_3)_2]$  to  $[NiX(PPh_3)_3]$  and biphenyl was observed at 298 K (Scheme 4(b)).<sup>24</sup> However, when isolated crystals of

*trans*- $[Ni(Ph)(X)(PPh_3)_2]$  were dissolved in toluene-*d*<sub>8</sub>, full decomposition of the sample was observed to occur within minutes, suggesting that the presence of  $PPh_3$  inhibits the decay of the nickel(II) complex. This is in contrast to observations made by Kochi, where the analogous complex with the smaller, more electron-rich triethylphosphine ligand (*i.e.*  $[Ni(Ar)X(PEt_3)_2]$ ) was found to be stable in solution at room temperature indefinitely.<sup>21</sup> This observation has been attributed to the better donor properties of triethylphosphine compared to triphenylphosphine meaning that triethylphosphine does not readily dissociate under the same conditions.

The mechanism of the decomposition of *trans*- $[Ni(Ph)X(PPh_3)_2]$  to  $[NiX(PPh_3)_3]$  and biphenyl was probed by conducting DFT calculations (Fig. 3).<sup>24</sup> The dissociation of triphenylphosphine from *trans*- $[NiCl(Ph)(PPh_3)_2]$  was proposed to be followed by a reaction with a second molecule of *trans*- $[NiCl(Ph)(PPh_3)_2]$  to form a chloride-bridge dinuclear intermediate. This dinuclear species could then lead to  $[NiCl_2(PPh_3)]$  and  $[Ni(Ph)_2(PPh_3)_2]$ , with reductive elimination of biphenyl from the latter species followed by comproportionation to form two molecules of  $[NiCl(PPh_3)_2]$  which then coordinate a third triphenylphosphine ligand. Alternatively, binuclear reductive elimination might form biphenyl and two nickel(I) species directly. These pathways were both found to be feasible thermodynamically, but some transition states were not located, and are indeed rather challenging to locate.

The reactions of  $[Ni(PCy_3)_2]$  with organohalides have been less well-studied, perhaps due to the need to prepare this complex from the reduction of the corresponding dihalide with reducing metals.<sup>25</sup> The oxidative addition of



**Scheme 4** (a) The reactions of  $[Ni(PPh_3)_4]$  with halobenzene substrates to form *trans*- $[Ni(Ph)X(PPh_3)_2]$  and  $[NiX(PPh_3)_3]$  complexes. (b) The decomposition of *trans*- $[Ni(Ph)X(PPh_3)_2]$  to form  $[NiX(PPh_3)_3]$  and biphenyl.<sup>24</sup>



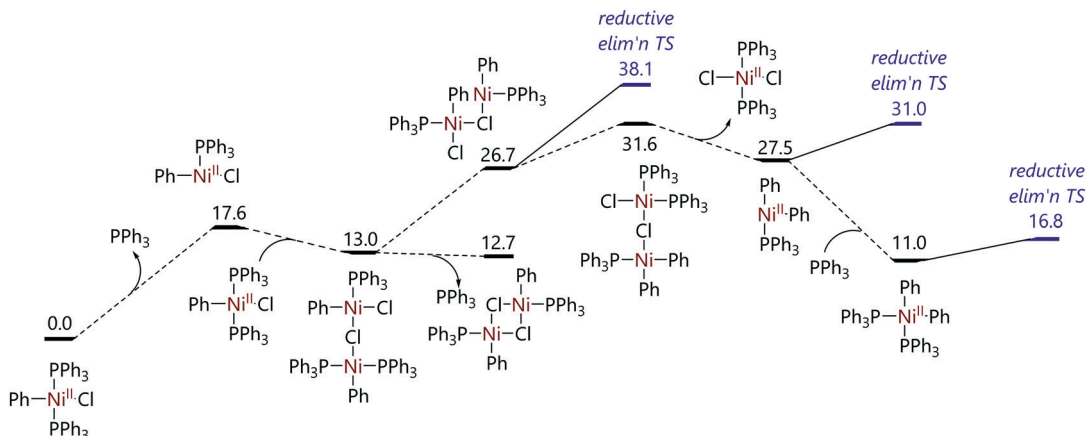


Fig. 3 Proposed pathway for the decomposition of *trans*-[NiCl(Ph)(PPh<sub>3</sub>)<sub>2</sub>] to [NiCl(PPh<sub>3</sub>)<sub>3</sub>].<sup>24</sup>

chloroarenes to [Ni(PCy<sub>3</sub>)<sub>2</sub>] is reported to lead to [Ni(Ar)Cl(PCy<sub>3</sub>)<sub>2</sub>] complexes, which decompose to form biphenyl and [NiCl(PCy<sub>3</sub>)<sub>2</sub>].<sup>26</sup> The corresponding reactions with alkyl halides lead to nickel(i) and nickel(ii) products and mixtures of alkanes and alkenes.

The oxidative addition reactions of nickel(0) complexes with bidentate ligands can often be complicated by catalyst speciation. Many such ligands lead to very stable four-coordinate [Ni(L)<sub>2</sub>] complexes that can be poorly reactive in catalysis.<sup>27</sup> As part of a comprehensive study of the trifluoromethylthiolation of aryl chlorides, Yin *et al.* screened several bidentate phosphines including XantPhos, (±)-BINAP, dppf, dcpf, dppm, dppe, and dppp (dppf = 1,1'-bis(diphenylphosphino)ferrocene; dcpf = 1,1'-bis(dicyclohexylphosphino)ferrocene; dppm = bis(diphenylphosphino)methane; dppe = 1,2-bis(diphenylphosphino)ethane; dppp = 1,3-bis(diphenylphosphino)propane). The latter three ligands and (±)-BINAP were ineffective, while XantPhos and the ferrocene derivatives gave moderate conversions; dppf was taken forward in the optimisation. Experimental studies established that [Ni(COD)<sub>2</sub>]/dppf reacts with aryl chlorides to form [NiCl(dppf)] as the ultimate product, while [Ni(COD)<sub>2</sub>]/dppe leads to poorly reactive [Ni(dppe)<sub>2</sub>]. Computational studies suggested a three centre concerted oxidative addition mechanism and confirmed the significant energy barrier to replacing a dppe ligand in [Ni(dppe)<sub>2</sub>] with chlorobenzene (33.1 kcal mol<sup>-1</sup>), explaining the poor reactivity of dppe-nickel species in the catalytic reaction. In addition, isolated [Ni(COD)(dppf)] performed better in catalysis than the same complex formed *in situ* by [Ni(COD)<sub>2</sub>]/dppf, suggesting an inhibitory role for COD.

Amatore and Jutand have generated coordinatively-unsaturated [Ni(dppe)] *in situ* from [NiCl<sub>2</sub>(dppe)] using electrochemical methods;<sup>28</sup> this decomposes to half an equivalent of [Ni(dppe)<sub>2</sub>] in the absence of organohalide but in the presence of bromobenzene it forms [NiBr(Ph)(dppe)]. The rate constant for oxidative addition is *ca.* 10<sup>5</sup> L mol<sup>-1</sup> s<sup>-1</sup>, consistent with the highly reactive nature of this bent, coordinatively-unsaturated species.

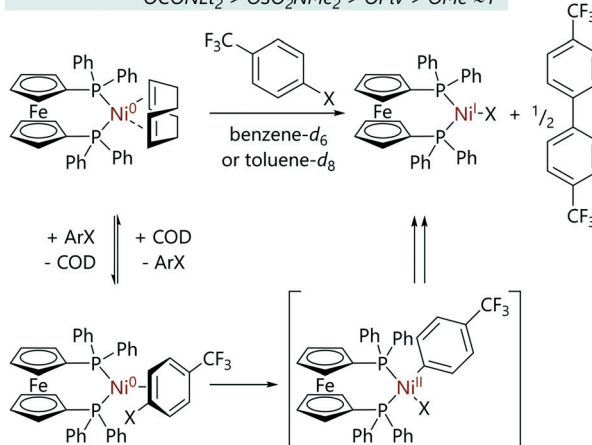
A study by Guard *et al.* in the same year noted the formation of [NiCl(dppf)] in reactions catalysed by dppf-nickel, regardless of the oxidation state of the (pre-)catalyst used or additional ligands present on that (pre-)catalyst.<sup>29</sup> The role of nickel(i) in catalysis is still a subject of active research and is beyond the scope of the present review. The comproportionation mechanism for dppf-nickel systems has been studied using DFT calculations.<sup>30</sup> It has been proposed that this comproportionation can be minimised by switching to bulkier 1,1-bis(dicyclohexylphosphino)ferrocene ligands.<sup>31</sup>

Nicolas *et al.* examined the oxidative addition of chloroarenes to [Ni( $\eta^2$ -C<sub>6</sub>H<sub>5</sub>Me)(dcpp)], in the context of nickel-catalysed Negishi cross-coupling reactions, using experimental and computational methodology (dcpp = 1,3-bis(dicyclohexylphosphino)propane).<sup>32</sup> [NiCl(Ar)(dcpp)] complexes were observed experimentally. Oxidative addition *via* a concerted transition state was found to have a rather low activation energy ( $\Delta G^\ddagger = 12.9$  kcal mol<sup>-1</sup>), with either transmetalation or the exchange of biaryl for chloroarene found to be the most energetically-demanding step. Lavoie *et al.* characterised a similar transition state for a [Ni(PAd-DalPhos)] species by DFT, and noted that it was similar in energy to oxidative addition to an analogous nickel(i) amide complex (PAd-DalPhos = 8-(2-(di-*o*-tolylphosphanyl)phenyl)-1,3,5,7-tetramethyl-2,4,6-trioxa-8-phosphaadamantane).<sup>33</sup>

Bajo *et al.* studied the reactions of model nickel complex [Ni(COD)(dppf)] with a bidentate phosphine ligand with aryl halides (and other aryl electrophiles).<sup>34</sup> It was previously known that these reactions lead to [NiX(dppf)] complexes as the final nickel-containing species. The oxidative addition reactions of various aryl electrophiles to [Ni(COD)(dppf)]<sup>35</sup> were monitored *via* <sup>31</sup>P NMR spectroscopy (Scheme 5). The reactions were found to be first order with respect to [Ni(COD)(dppf)] and aryl halide, and were inhibited by added COD. On the basis of the kinetic data, an initial reversible displacement of COD with aryl halide was proposed, followed by an irreversible oxidative addition step. The nickel(ii) oxidative addition product – *i.e.* [Ni(Ar)X(dppf)] – typically



Reaction Rate:  $I > Br > Cl > OTs > OCO_2Et > OTf > OCONet_2 > OSO_2NMe_2 > OPiv > OMe \approx F$



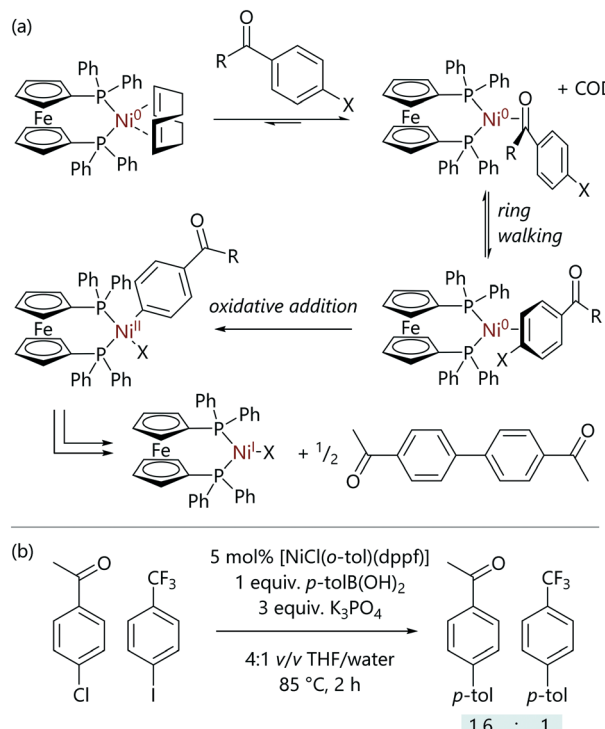
Scheme 5 The oxidative addition of aryl halides and other aryl electrophiles to  $[\text{Ni}(\text{COD})(\text{dppf})]$ .<sup>34</sup>

underwent rapid comproportionation with  $[\text{Ni}(\text{COD})(\text{dppf})]$  to form  $[\text{NiX}(\text{dppf})]$  which was the only nickel-containing product observed; these species were characterised using EPR spectroscopy and single crystal X-ray diffraction analysis. Notably, comproportionation was sufficiently fast that no oxidative addition products were observed in the  $^{31}\text{P}$  NMR spectra at ambient temperatures. The oxidative addition product was observed as two doublets in the  $^{31}\text{P}$  NMR spectra at lower temperatures and when more sterically-hindered *ortho*-substituted aryl halides were employed as substrates.

It was also noted that naphthyl substrates are much more reactive than aryl substrates in oxidative addition to  $[\text{Ni}(\text{COD})(\text{dppf})]$  (by *ca.* six- to eight-fold).<sup>34</sup> This is consistent with the observation that studies that involve very challenging substrates such as aryl ethers tend to demonstrate higher yields with naphthyl and other extended aromatic systems.

Three mechanisms previously proposed for oxidative addition of aryl halides to nickel(0) and palladium(0) complexes were considered. Radical reactions were ruled out as the addition of TEMPO had no impact on the rates of oxidative addition; however, subsequent studies have shown that TEMPO is not always a reliable radical probe in this system as it can react directly with nickel(0).<sup>36</sup> The activation parameters obtained were similar to those for the oxidative addition of aryl halides to  $[\text{Pd}(\text{PPh}_3)_4]$ .<sup>37</sup> Notably, the Hammett plot obtained by Bajo *et al.* showed that for electron-rich substrates  $\rho = 1.2$  whereas electron-poor substrates appeared to show an opposing trend, consistent with a change in rate-determining step. The shallow gradients obtained from the Hammett plots ruled out an  $S_{\text{N}}\text{Ar}$ -type mechanism<sup>7</sup> and a small  $\Delta S^\ddagger$  of  $0(3)$  cal  $\text{K}^{-1}$   $\text{mol}^{-1}$  led to a three-centre transition state being proposed (see Scheme 1).

Following on from this study, Cooper *et al.* have investigated how common functional groups can interact



Scheme 6 (a) Ring-walking processes in the oxidative addition of aryl halides with aldehyde and ketone functional groups to  $[\text{Ni}(\text{COD})(\text{dppf})]$ . (b) The effect of aldehyde and ketone coordination on selectivity in Suzuki–Miyaura cross-coupling reactions.<sup>38</sup>

with nickel(0) complexes and influence the rate and selectivity of oxidative addition (Scheme 6);<sup>38</sup> model nickel complexes with dppf ligands were utilised, and were compared to the analogous palladium complexes in Suzuki–Miyaura cross-coupling reactions.<sup>39</sup> Aldehyde- and ketone-substituted aryl chlorides underwent unexpectedly rapid oxidative addition to  $[\text{Ni}(\text{COD})(\text{dppf})]$ . The kinetic data obtained implied that the previously described three-centred concerted mechanism was in operation;<sup>34</sup> however, the initial ligand exchange (aryl halide for COD) was thought to be favoured when the aryl halide bears an aldehyde or ketone, shifting the initial equilibrium towards the  $[\text{Ni}(\eta^2\text{-ArX})(\text{dppf})]$  complex. Aldehydes and ketones are known to be excellent ligands for low valent nickel complexes,<sup>40–43</sup> with nickel complexes that bear a bidentate phosphine ligand (typically dtbpe) giving rise to some interesting electronic effects that have been examined in detail by Kennepohl and Love (dtbpe = 1,2-di(*tert*-butylphosphino)ethane).<sup>44,45</sup> Amides and esters did not benefit from this coordination effect. In the reaction between  $[\text{Ni}(\text{COD})(\text{dppf})]$  and 4-chlorobenzaldehyde, an intermediate was observed that presented two doublets in the  $^{31}\text{P}$  NMR spectrum; these were attributed to the  $\eta^2(\text{CO})$ -complex.

This exceptional reactivity of aromatic halides bearing aldehyde and ketone groups was then exploited to achieve selective Suzuki–Miyaura cross-coupling reactions;<sup>38</sup> in inter- and intramolecular competition experiments, selective cross-



coupling was achieved at the site that was in conjugation with the aldehyde or ketone. This selectivity was such that the normal order of reactivity of aryl halides ( $I > Br > Cl$ ) could be overturned, and was attributed to a ‘ring-walking’ process where the nickel moves from the initial site of coordination across a  $\pi$ -system to the aryl halide.<sup>46–51</sup> This proposal was supported by DFT calculations.

However, aldehydes and ketones (without halide functional groups) can act as inhibitors in these reactions, which prevents a potential drawback to the use of nickel catalysis.<sup>38</sup> Palladium has been shown not to interact strongly enough to induce these selectivity and inhibition effects observed with nickel.<sup>39</sup>

In light of the much wider scope of electrophiles that are reactive with nickel in cross-coupling catalysis,<sup>15,52</sup> there can be selectivity challenge in nickel catalysis if the substrate is highly functionalised. Two recent studies have explored these selectivity challenges in some detail.

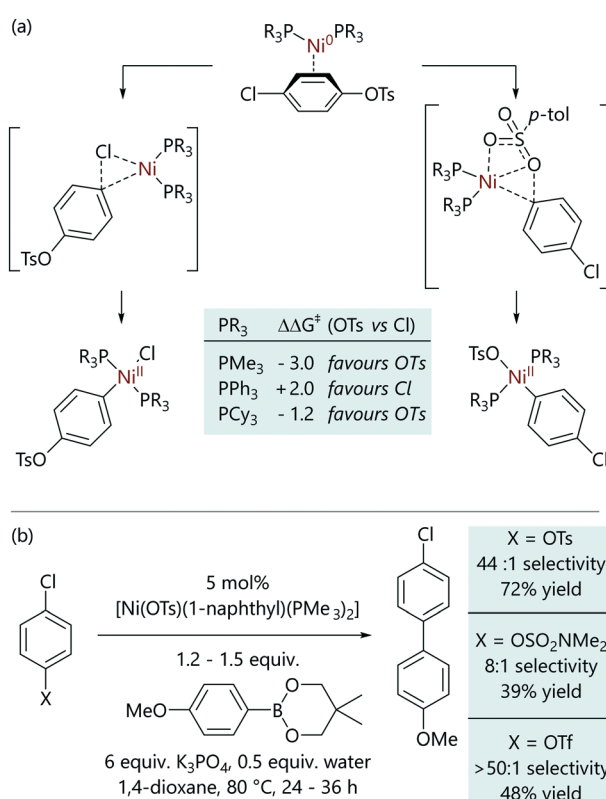
Entz and Russell *et al.* examined the case of C-Cl *versus* C-OTs activation in nickel-catalysed Suzuki–Miyaura cross-coupling reactions using a combination of experiment and theory.<sup>53</sup> Bajo *et al.* had previously shown that the oxidative addition of *p*-F<sub>3</sub>CC<sub>6</sub>H<sub>4</sub>Cl to [Ni(COD)(dppf)] was *ca.* three

times faster than the corresponding reaction with *p*-F<sub>3</sub>CC<sub>6</sub>H<sub>4</sub>OTs.<sup>34</sup> Computational studies of the reaction of 4-chlorophenyl tosylate were conducted initially using model species [Ni(PMe<sub>3</sub>)<sub>2</sub>], [Ni(PPh<sub>3</sub>)<sub>2</sub>], and [Ni(PCy<sub>3</sub>)<sub>2</sub>] and  $\Delta\Delta G^\ddagger$  (*i.e.*  $\Delta G_{\text{OTs}}^\ddagger - \Delta G_{\text{Cl}}^\ddagger$ ) was evaluated in each case (Scheme 7(a)).<sup>53</sup> It was noted that the trimethylphosphine complex ought to prefer C-OTs oxidative addition ( $\Delta\Delta G^\ddagger = -3.0$ ) while the triphenylphosphine complex should prefer C-Cl activation ( $\Delta\Delta G^\ddagger = +2.0$ ) and the tricyclohexylphosphine complex should be less selective ( $\Delta\Delta G^\ddagger = -1.2$ ). The structures of the (concerted) oxidative addition transition states revealed favourable interactions between the oxygen of the sulfonate and the nickel centre in the oxidative addition of the tosylate; these were more pronounced for trimethylphosphine due to its smaller steric impact.

Experimental studies in which [Ni(COD)<sub>2</sub>] plus a phosphine ligand were exposed to a 1:1 mixture of 1-chloronaphthalene and naphthyl 1-tosylate allowed the corresponding oxidative addition products to be observed by <sup>31</sup>P{<sup>1</sup>H} NMR spectroscopy, and thus for their ratio to be measured.<sup>53</sup> Triarylphosphines and the bidentate dcpf ligand were overwhelmingly selective for C-Cl oxidative addition, while trialkylphosphines and arylalkylphosphines produced mixtures. Dimethylphenylphosphine and trimethylphosphine were the only ligands that were selective for C-OTs oxidative addition (in ratios of 1:5.7 and 1:6.3, respectively). This then led to the development of cross-coupling conditions that allowed a range of chloro/tosylate, chloro/triflate, and chloro/sulfamate substrates to be selectively coupled at the C-O site, leaving the aryl chloride intact for further reactions (Scheme 7(b)).

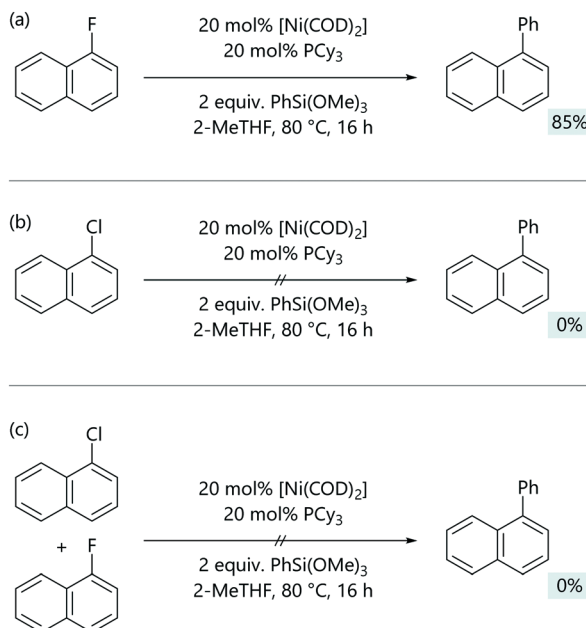
Jacobs and Keaveney exploited the reversibility of C-Cl bond activation and the different reactivity of arylnickel(II) fluorides and arylnickel(II) chlorides to achieve C-F selective Hiyama coupling reactions.<sup>54</sup> [Ni(Ar)Cl(PR<sub>3</sub>)<sub>2</sub>] complexes will not react directly with silanes, while [Ni(Ar)F(PR<sub>3</sub>)<sub>2</sub>] complexes can.<sup>55</sup> A Hiyama cross-coupling between 1-fluoronaphthalene and trimethoxyphenylsilane was achieved employing [Ni(COD)<sub>2</sub>]/PCy<sub>3</sub> as the catalytic system (Scheme 8). Notably, under these optimised conditions, no conversion was observed for 1-chloronaphthalene. In a competition experiment with both 1-fluoronaphthalene and 1-chloronaphthalene present, no coupled product was observed.

DFT calculations were used to gain insight into the mechanism of this reaction.<sup>54</sup> Optimisation experiments suggested a [Ni(PCy<sub>3</sub>)] active species, as an increase in the ligand to nickel ratio led to a decrease in the yield, and so the calculated free energy profile started from [Ni(COD)(2-MeTHF)(PCy<sub>3</sub>)] ( $G_{\text{rel}} = 0$ ). As expected, the barrier for the concerted oxidative addition of 1-fluoronaphthalene ( $G_{\text{rel}} = 28.4$  kcal mol<sup>-1</sup>) was much higher than that for 1-chloronaphthalene ( $G_{\text{rel}} = 8.0$  kcal mol<sup>-1</sup>). For transmetalation, a low energy transition state could be located for the Ni-F pathway ( $G_{\text{rel}} = 2.1$  kcal mol<sup>-1</sup>), but transmetalation was much more energetically demanding for



**Scheme 7** (a) Oxidative addition transition states for the possible reactions of 4-chlorophenyl tosylate with [Ni(PR<sub>3</sub>)<sub>2</sub>] complexes. (b) Examples of selective cross-coupling at the C-O bond in the presence of a C-Cl bond, enabled by the use of a trimethylphosphine–nickel pre-catalyst; selectivity was determined by GC analysis, while yields are isolated yields.<sup>53</sup>



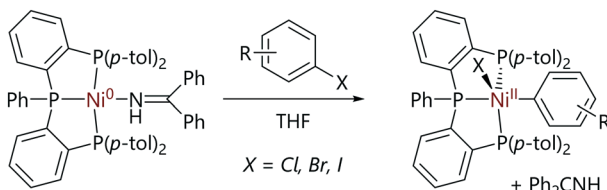


**Scheme 8** (a) The base-free Hiyama coupling of aryl fluorides. (b) Chloroarenes are unreactive under the same conditions, because the arylnickel(II) chloride cannot directly transmetalate. (c) Chloroarenes poison the otherwise productive reactions of fluoroarenes.<sup>54</sup>

the Ni-Cl pathway ( $>50$  kcal mol $^{-1}$ ). Consistent with the experimental observations from the competition reaction, the irreversible oxidative addition with 1-chloronaphthalene is faster than reaction with 1-fluoronaphthalene and forms the oxidative addition product ( $G_{\text{rel}} = -26.1$  kcal mol $^{-1}$ ) which ultimately inhibits cross-coupling.

Developing a catalyst system to promote reversible C-Cl oxidative addition would induce the desired selectivity for reaction at the C-F bond over reaction at the C-Cl bond. Whilst the oxidative addition of 1-fluoronaphthalene does not proceed if the ligand is too bulky, the reversible oxidative addition of 1-chloronaphthalene required a bulky ligand.<sup>54</sup> The contradictory results encountered meant that the desired selectivity for C-F over C-Cl oxidative addition is difficult to achieve, however the concept of selectively destabilising the C-Cl oxidative addition product is a promising avenue for future work.

Pérez-García *et al.* have studied the reactions of nickel(0) complexes with a tris(phosphine) ligand (Scheme 9).<sup>56</sup> The treatment of the nickel(0) complex with haloarenes led to the formation of well-defined nickel(II) oxidative addition



**Scheme 9** Oxidative addition reactions of a tris(phosphine)nickel(0) complex.<sup>56</sup>

products, of which one example was structurally characterised by X-ray diffraction analysis.

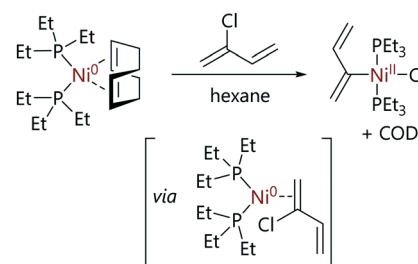
Kinetic studies were carried out in the presence of excess imine ligand and aryl bromide revealed kinetic behaviour that was pseudo-first order in the nickel complex, first order in aryl halide, and inverse first order in imine. This is consistent with a pre-equilibrium in which the imine ligand is exchanged for the aryl halide before oxidative addition. A Hammett correlation (using  $\sigma$  substituent constants) revealed a significant and positive reaction constant ( $\rho = 2.6$ ), which is consistent with a three-centre oxidative addition transition state, although it is not possible to decouple the electronic effects on the pre-equilibrium from the electronic effects on the transition state energy. An Eyring analysis yielded a negative entropy of activation ( $\Delta S^\ddagger = -18(2)$  cal K $^{-1}$  mol $^{-1}$ ), suggesting an associative ligand exchange prior to oxidative addition. DFT calculations revealed that a three-centre concerted oxidative addition mechanism was reasonable, with halide abstraction being much less favourable ( $\Delta\Delta G^\ddagger = +7.2$  kcal mol $^{-1}$ ).

### Reactions with vinyl halides

Relatively few studies into the mechanism of oxidative addition of vinyl halides to nickel have been carried out. This may be due to the difficult synthesis and the ultimate stability of complex vinyl halides, as studies that have been conducted have utilised simple halides.

Fahey has studied the oxidative addition of vinyl halides to nickel complexes.<sup>18,57</sup> Vinyl bromide and chloroprene reacted rapidly with  $[\text{Ni}(\text{COD})(\text{PET}_3)_2]$  to give the corresponding halo-organo-nickel complexes. The product from oxidative addition of the vinyl bromide decomposed at ambient temperatures and therefore was not subjected to full characterisation. However, the nickel product from the oxidative addition of the chloroprene was stable under argon for months and was fully characterised as the *trans*-allyl nickel complex (Scheme 10).

The proposed mechanism for the reaction of  $[\text{Ni}(\text{COD})(\text{PET}_3)_2]$  with vinyl halides suggest a coordination of the  $\pi$ -system to nickel(0) followed by formation of the oxidative addition product (Scheme 10).<sup>57</sup> The intermediates in this mechanism were not isolated and therefore the mechanism was speculative but it may be similar to the ring-walking



**Scheme 10** Reaction of  $[\text{Ni}(\text{COD})(\text{PET}_3)_2]$  with chloroprene to form a stable allyl product.<sup>57</sup>



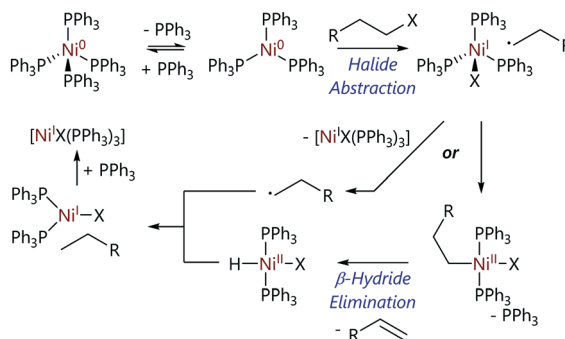
processes known to occur with nickel complexes (*vide supra*). Radical processes were ruled out for vinyl substrates; vinyl radicals exhibit very poor stability, but more importantly the stereochemistry was retained when *trans*- $\beta$ -bromostyrene was used as a substrate for oxidative addition. While no rate constants were measured, it was noted that vinyl halides reacted rapidly with  $[\text{Ni}(\text{COD})(\text{PET}_3)_2]$ , while aryl halides required elevated temperatures of 50–60 °C.

### Reactions with alkyl halides

Stille and Cowell have studied the reactions of benzyl halides with  $[\text{Ni}(\text{PPh}_3)_4]$  as part of efforts to develop methodology for the formation of esters by alkoxycarbonylation.<sup>58</sup> They noted poor stereochemical control of substrates where the benzylic centre had point stereochemistry, which is suggestive of (planar) radical intermediates; in addition, compounds with hydrogen atoms at the adjacent position were affected by  $\beta$ -hydride elimination.

Zhang *et al.* utilised a nickel(0) complex with tetradentate  $\text{P}_2\text{S}_2$  ligand (*o*-(Ph<sub>2</sub>P)C<sub>6</sub>H<sub>4</sub>CH<sub>2</sub>SCH<sub>2</sub>)<sub>2</sub>) for a reactivity study with allyl and alkyl halides (in the presence of NaBPh<sub>4</sub>).<sup>59</sup> Oxidative addition to allyl halides led to cationic allylnickel(II) species. The reactions with alkyl halides produced  $[\text{Ni}-\text{R}]^+$  complexes, which underwent  $\beta$ -hydride elimination to form nickel(II) hydride complexes.

Kehoe *et al.* used variable temperature NMR spectroscopy to elucidate the mechanism of oxidative addition of various alkyl halides to  $[\text{Ni}(\text{PPh}_3)_4]$ .<sup>60</sup> The <sup>31</sup>P NMR spectrum of  $[\text{Ni}(\text{PPh}_3)_4]$  at room temperature contains a single broad resonance ( $\delta_{\text{P}} = 24$  ppm). When cooled to 200 K, the spectrum contains two resonances ( $\delta_{\text{P}} = 8, 25$  ppm) which are attributed to free PPh<sub>3</sub> and  $[\text{Ni}(\text{PPh}_3)_3]$ , respectively, confirming that the dominant species in the reaction mixture is  $[\text{Ni}(\text{PPh}_3)_3]$ ;  $K_{\text{eq}}$  for this dissociation is  $>10^6 \text{ mol L}^{-1}$ .<sup>20</sup> The reaction of  $[\text{Ni}(\text{PPh}_3)_3]$  with iodoalkanes yielded alkanes and alkenes as the major products, plus a nickel hydride as the minor product (Scheme 11). This product ratio suggested oxidative addition was occurring followed by a subsequent  $\beta$ -H elimination event. The observation that the rate decreases in the order *t*-BuX > *s*-BuX > *n*-BuX (X = Cl, Br, I) is consistent with a radical mechanism. Experimental

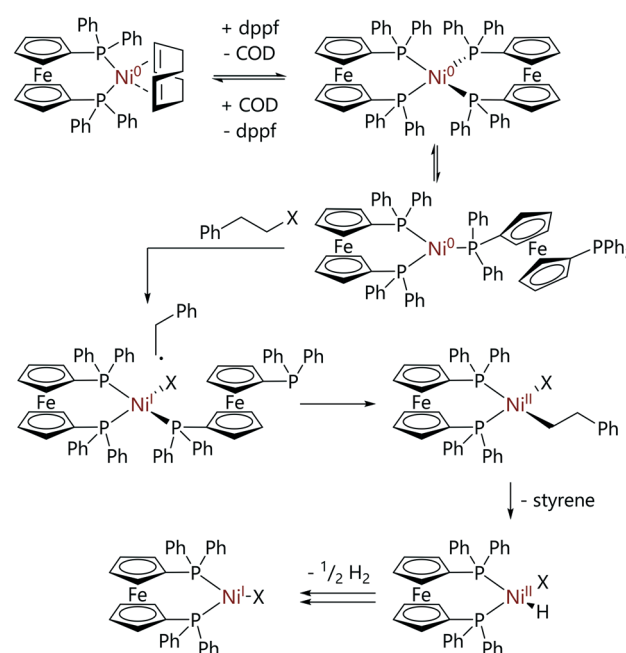


Scheme 11 Proposed mechanism for the reactions of alkyl halides with  $[\text{Ni}(\text{PPh}_3)_4]$ .<sup>60</sup>

evidence, plus evidence from previous work published by Tsou and Kochi,<sup>21</sup> led to halide abstraction being proposed as the mechanism of reaction, which is followed by a subsequent  $\beta$ -H elimination step.

The low concentrations of the nickel hydride complex found in the reaction mixtures prompted further investigation to determine how this was being consumed.<sup>60</sup> It was established that alkyl radicals have the ability to escape the cage and do not necessarily all recombine to form the formal (Ni<sup>II</sup>) oxidative addition product. These radicals have three preferred reactions: self-reaction, disproportionation (to form alkane plus alkene), or abstraction of a proton from either the solvent or nickel hydride complex. Equal amounts of alkene and alkane products, consistent with disproportionation, were observed; however, a lack of longer chain alkanes that would be consistent with combination reactions ruled out self-combination. There was also no evidence of any deuterated products, ruling out hydrogen atom abstraction from solvent molecules (reactions were carried out in toluene-*d*<sub>8</sub>). The conclusion was that the alkyl radicals escaping from the cage were reacting preferentially with the nickel hydride, and this was supported using DFT calculations, providing an explanation for the low concentrations of nickel hydrides observed.

Greaves *et al.* explored the mechanism of the reaction of  $[\text{Ni}(\text{COD})(\text{dppf})]$  with (2-haloethyl)benzene substrates.<sup>36</sup> In contrast to the analogous reactions with aryl halides, these reactions proceeded *via*  $[\text{Ni}(\text{dppf})_2]$ , a species which exists in equilibrium ( $K_{\text{eq}} = 6.8$ ) with  $[\text{Ni}(\text{COD})(\text{dppf})]$  and excess dppf. The reactions of these alkyl halides with  $[\text{Ni}(\text{COD})(\text{dppf})]$ , in the presence of dppf, were monitored by <sup>31</sup>P NMR spectroscopy. Reactions were first order with respect to



Scheme 12 Proposed mechanism for the reactions of alkyl halides with  $[\text{Ni}(\text{COD})(\text{dppf})]$ .<sup>36</sup>

[Ni(COD)(dppf)], dppf and alkyl halide, and showed an inverse first order dependence on COD concentration. A product study revealed that [NiX(dppf)] was the final nickel-containing product, and this was detected by EPR spectroscopy. The evolution of dihydrogen was confirmed by  $^1\text{H}$  NMR spectroscopy and the presence of styrene was confirmed by GC-MS analysis. A reaction mechanism that explains the observed products was proposed (Scheme 12). An initial reversible displacement of COD with dppf yielded the active species [Ni(dppf)<sub>2</sub>], which then undergoes halide abstraction and radical recombination to form [Ni(CH<sub>2</sub>CH<sub>2</sub>-Ph)X(dppf)] (not observed by  $^{31}\text{P}$  NMR spectroscopy). A  $\beta$ -H elimination event followed by dissociation of styrene yields [Ni(H)(X)(dppf)] which undergoes comproportionation to form [NiX(dppf)] and dihydrogen.

The involvement of radicals in the reaction was confirmed as reaction rates dramatically increased when *tert*-butyl bromide or (2-bromopropyl)benzene were employed as substrates; these reactions were too fast to monitor by NMR spectroscopy.<sup>36</sup> There were two mechanistic possibilities: outer sphere electron transfer and halide abstraction. Outer sphere electron transfer was ruled out as a mechanistic possibility, as [Ni(dppe)<sub>2</sub>], which should be capable of outer sphere electron transfer, did not undergo reaction with the (2-haloethyl)benzene substrates. DFT calculations confirmed a halide abstraction mechanism was most likely for these reactions, operating *via* a [Ni(dppf)<sub>2</sub>] active species.

## Nickel(0) complexes with chelating nitrogen ligands

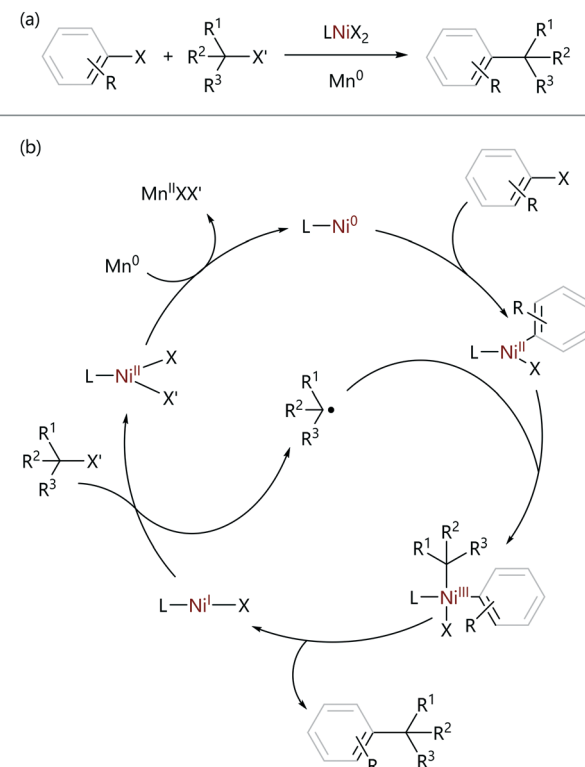
The reactions of nickel(0) complexes with bipyridine ligands (or similar) are arguably far less well understood than for other ligand classes. There is an emerging picture that suggests that, because these ligands are redox non-innocent, nickel(i)<sup>61</sup> plays a more significant role in the corresponding catalytic reactions.<sup>62,63</sup> Vicic has studied the terpyridine systems in some detail, revealing that many [NiX(terpy)] complexes – which on inspection appear to be nickel(i) – are in fact better described as nickel(ii) with a radical on the ligand (terpy = 2,2':6',2"-terpyridine);<sup>64,65</sup> a full and detailed discussion of that work is somewhat beyond the scope of this review – which focusses on nickel(0) – but interested readers are directed towards the relevant manuscripts.

The reported reactivity of this class of nickel(0) complex with aryl halides typically leads to the invocation of odd-numbered oxidation states, although some two-electron (oxidative addition) reactivity has also been noted. For example, Shields and Doyle reported the synthesis of diamagnetic square planar complexes [NiCl(*o*-tol)(dtbpy)] and [NiCl(*p*-tol)(dtbpy)] from the reaction of [Ni(COD)<sub>2</sub>], dtbpy, and the corresponding chloroarene in THF (dtbpy = 4,4-di(*tert*-butyl)bipyridine);<sup>66</sup> these structures were supported by  $^1\text{H}$  and  $^{13}\text{C}$  NMR data and elemental analysis.

Weix used the observed difference in reactivity between aryl and alkyl halides to achieve the selective  $\text{sp}^2$ - $\text{sp}^3$

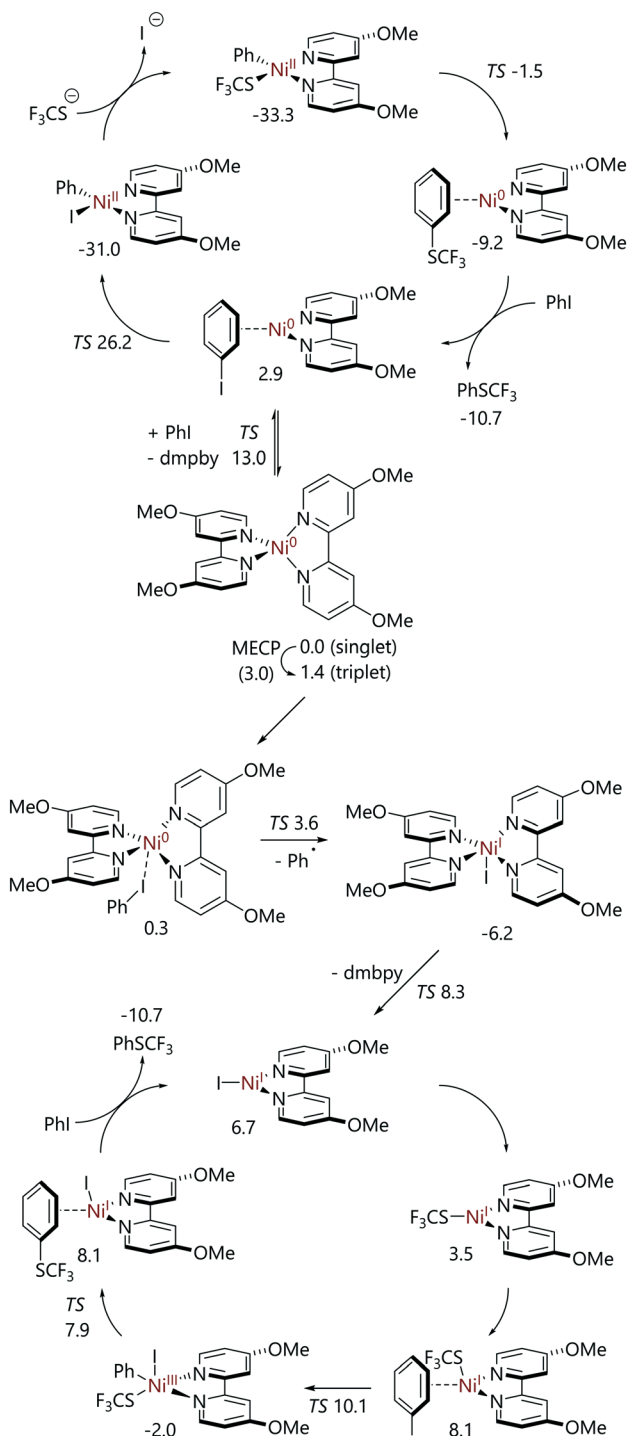
reductive cross-electrophile coupling reactions of aryl halides with alkyl halides;<sup>4,67</sup> these reactions employ a Ni<sup>II</sup> pre-catalyst, and use an external reductant to form the active Ni<sup>0</sup> species *in situ*. In most cases, the ligands are substituted bipyridine or phenanthroline ligands. The oxidative addition of the aryl halide is selectively achieved (*versus* the reaction of the alkyl halide) due to a difference in rate. This arylnickel(ii) intermediate was found to stoichiometrically react with alkyl halides to re-form the initial pre-catalyst, without the requirement for an external reductant. Radical-clock experiments carried out using (cyclopropyl)methyl bromide as the alkyl halide confirmed the presence of radical intermediates, as only the ring-opened product was observed.<sup>68</sup> Increased amounts of ring-opened product were observed when the nickel concentration was increased, suggesting radical formation and reaction were occurring at different points of the catalytic cycle. Finally, from an analysis of the products of quenched reaction mixtures, the oxidative addition product was found to be the resting state of the catalyst explaining the selectivity of the reaction. These observations result in the proposed catalytic cycle shown in Scheme 13.

Kalvet *et al.* and Jover have both examined the nickel-catalysed trifluoromethylthiolation of aryl halides using DFT calculations.<sup>62,63</sup> Jover has conducted a DFT study of the alternative full cycles for the trifluoromethylthiolation reaction of iodobenzene catalysed by 4,4'-di(methoxy)-2,2'-



**Scheme 13** (a) Reductive cross-electrophile cross-coupling reactions. (b) The proposed mechanism for the reductive cross-electrophile coupling reactions of  $\text{sp}^2$ - and  $\text{sp}^3$ -organohalides.<sup>4,67</sup>





**Scheme 14** Catalytic cycles for iodobenzene trifluoromethylthiolation catalysed by  $[\text{Ni}(\text{dmbpy})_2]$ , as determined from DFT calculations.<sup>63</sup>

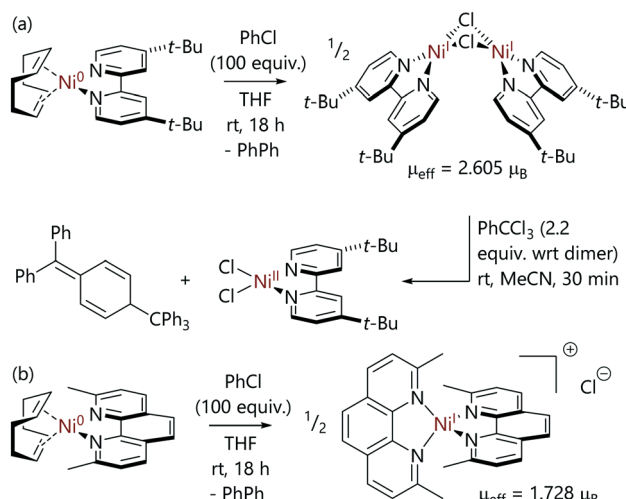
bipyridine (dmbpy) ligated nickel(0) (Scheme 14).<sup>63</sup> Two pathways from  $[\text{Ni}(\text{dmbpy})_2]$  were considered. The first was oxidative addition *via* a three-centre transition state, followed by transmetalation and reductive elimination (*i.e.* a  $\text{Ni}^0/\text{Ni}^{\text{II}}$  cycle). The second was halide abstraction on the triplet surface to form a nickel(i) species that then mediates a  $\text{Ni}^{\text{I}}/\text{Ni}^{\text{III}}$  cycle proceeding *via* transmetalation, oxidative addition,

and reductive elimination. For the  $\text{Ni}^0/\text{Ni}^{\text{II}}$  cycle, the highest energy structure was the oxidative addition transition state at 26.3 kcal mol<sup>-1</sup> vs.  $[\text{Ni}(\text{dmbpy})_2]$ . However, the formation of  $[\text{NiI}(\text{dmbpy})]$  from  $[\text{Ni}(\text{dmbpy})_2]$  is facile; this occurs *via* a minimum energy crossing point from the singlet surface to the triplet surface ( $G_{\text{rel}} = 3.0$  kcal mol<sup>-1</sup>), halide abstraction ( $G_{\text{rel}} = 3.6$  kcal mol<sup>-1</sup>), and then ligand dissociation from  $[\text{NiI}(\text{dmbpy})_2]$  ( $G_{\text{rel}} = 8.3$  kcal mol<sup>-1</sup>).

While  $[\text{NiI}(\text{dmbpy})]$  is 6.7 kcal mol<sup>-1</sup> higher in energy than  $[\text{Ni}(\text{dmbpy})_2]$  plus iodobenzene, the  $\text{Ni}^{\text{I}}/\text{Ni}^{\text{III}}$  catalytic cycle that it can mediate features very low barriers, with the slowest step being oxidative addition to  $[\text{Ni}(\text{SCF}_3)(\text{dmbpy})]$  ( $G_{\text{rel}} = 10.1$  kcal mol<sup>-1</sup>).

Mohadjer Beromi *et al.* have studied the reactions of aryl halides with bipyridine-nickel(0) and phenanthroline-nickel(0) complexes that were formed *in situ* (Scheme 15).<sup>9</sup> In the case of the 4,4'-di(*tert*-butyl)-2,2'-bipyridine (dtbbpy) complex, the reaction of  $[\text{Ni}(\text{COD})(\text{dtbbpy})]$  with excess chlorobenzene led to  $[\text{Ni}(\mu\text{-Cl})(\text{dtbbpy})]_2$  which was characterised by methods including NMR spectroscopy and X-ray crystallography;<sup>9</sup> its magnetic moment was found to be  $2.605\mu_{\text{B}}$  (Evans's method). This dimer is EPR silent, and so cannot be detected or characterised using EPR spectroscopy. It can either be described as two ferromagnetically-coupled nickel(i) centres or as two nickel(ii) centres with radical anion ligands; XPS data are consistent with a +2 oxidation state at nickel. This dimer could be converted to  $[\text{NiCl}_2(\text{dtbbpy})]$  using trityl chloride, which formed Gomberg's dimer as the byproduct. Alternatively, reactions with 2,4,6-trialkylphenylmagnesium bromide generated  $[\text{Ni}(\text{Ar})_2(\text{dtbbpy})]$  complexes.

In contrast, the reactions of neocuproine (2,9-dimethyl-1,10-phenanthroline, neoc) complex  $[\text{Ni}(\text{COD})(\text{neoc})]$ <sup>69</sup> with excess chlorobenzene resulted in the formation of monomeric nickel(i) complex  $[\text{Ni}(\text{neoc})]_2\text{Cl}$ , which has an outer sphere chloride counterion ( $\mu_{\text{eff}} = 1.728\mu_{\text{B}}$ ).<sup>9</sup> This



**Scheme 15** Reactions between  $[\text{Ni}(\text{COD})(\text{L})]$  complexes and chlorobenzene, where  $\text{L}$  is (a) a bidentate bipyridine or (b) a 2,9-dimethylphenanthroline ligand.<sup>9</sup>

species was characterised by techniques including EPR spectroscopy. The outcomes of these reactions are therefore quite sensitive to ligand structure.

## Nickel(0) complexes with N-heterocyclic carbene ligands

There is significant interest in the use of N-heterocyclic carbenes as ligands for nickel catalysis, especially for the activation of stronger bonds such as those in aryl ethers. The synthesis of NHC-bearing nickel catalysts<sup>70</sup> and their applications in a variety of catalytic reactions<sup>71,72</sup> have recently been reviewed. Nickel(0) complexes with one or two NHC ligands have been shown to react with organohalides *via* one or two electron steps.

There are relatively few well-defined nickel(0) complexes with a single NHC ligand, and these are largely limited to  $[\text{Ni}(\text{NHC})(\eta^2, \eta^2\text{-1,6-hexadiene})]$ ,<sup>73</sup>  $[\text{Ni}(\text{NHC})(\eta^6\text{-arene})]$ ,<sup>74</sup> and  $[\text{Ni}(\text{NHC})(\eta^2\text{-olefin})_2]$ <sup>75-77</sup> complexes.  $[\text{Ni}(\text{IPr})(\eta^2, \eta^2\text{-1,6-hexadiene})]$  was found to react with allyl chlorides to form well-defined  $[\text{Ni}(\text{allyl})\text{Cl}(\text{IPr})]$  complexes (IPr = 1,3-bis(2,6-di(iso-propyl)phenyl)imidazol-2-ylidene).<sup>73</sup>

De Aguirre *et al.* have modelled each step of a tandem photocatalysis/cross-coupling reaction in which 2-iodoacetamide and 1-octene are converted to the corresponding indoline (Fig. 4).<sup>78</sup> The catalyst formed *in situ* (from  $[\text{Ni}(\text{COD})_2]$  plus IPr) was proposed to be  $[\text{Ni}(\text{IPr})(\eta^2\text{-1-octene})]$ ; halide abstraction to form  $[\text{Ni}(\text{I})(\text{IPr})(\eta^2\text{-1-octene})]$  plus an aryl radical was found to be significantly more energetically favourable than oxidative addition ( $\Delta\Delta G^\ddagger = 13.7$  kcal mol<sup>-1</sup>). The remainder of the work led the authors to conclude that a  $\text{Ni}^0/\text{Ni}^{\text{I}}/\text{Ni}^{\text{II}}/\text{Ni}^{\text{III}}$  mechanism was operative for this reaction.

Nicasio and Maseras have mapped out the Buchwald–Hartwig cross-coupling reactions of heteroaryl halides catalysed by  $[\text{Ni}(\text{IPr})(\eta^2\text{-styrene})_2]$  (Fig. 5).<sup>79</sup> The reactions of

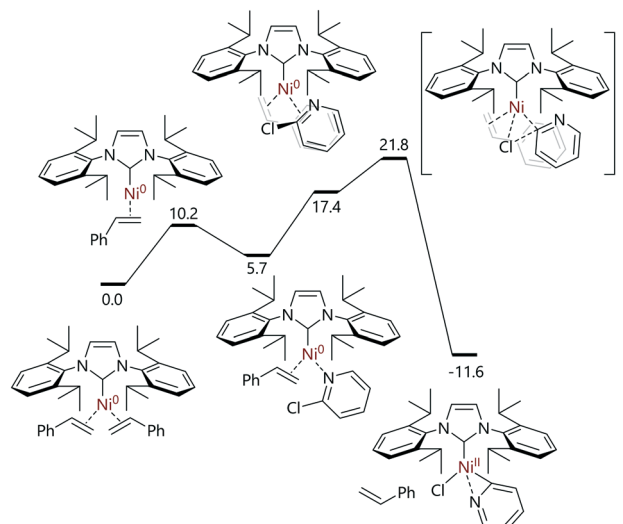


Fig. 5 Oxidative addition as the first step in the  $[\text{Ni}(\text{IPr})(\eta^2\text{-styrene})_2]$ -catalysed amination of (hetero)aryl halides.<sup>79</sup>

2-chloropyridine with  $[\text{Ni}(\text{IPr})(\eta^2\text{-styrene})_2]$  or  $[\text{Ni}(\eta^2\text{-C}_6\text{H}_5\text{Me})(\text{IPr})]$  led to a 2:3 mixture of two nickel(II) complexes: a nickel monomer bound to the nitrogen and C2 of pyridine, and another in which two 2-pyridyl units bridge two nickel centres. Both structures were characterised using a number of techniques, including single crystal X-ray diffraction analysis. The use of 2-chloro-6-*tert*-butylpyridine prevented the formation of a 2-pyridyl-bridged species, and allowed the isolation of the monomeric complex. DFT analysis of this reaction pathway suggested that the reaction proceeded *via* the dissociation of (only) one styrene ligand, followed by coordination of 2-chloropyridine *via* the nitrogen atom. Rearrangement to an  $\eta^2$ -complex and oxidative addition (*via* an  $S_{\text{N}}2$ -type transition state) delivers the experimentally-observed  $[\text{Ni}(\text{IPr})(\kappa^2\text{-N,C-2-pyridyl})]$  complex; a halide abstraction transition state was not located computationally, but it was noted that the halide abstraction step would produce products that were higher in energy by *ca.* 20 kcal mol<sup>-1</sup> ( $G_{\text{rel}} = 8.2\text{--}12.7$  kcal mol<sup>-1</sup>).

In contrast, the reaction of 3-chloropyridine with  $[\text{Ni}(\eta^2\text{-C}_6\text{H}_5\text{Me})(\text{IPr})]$  produced a trimeric  $[\text{NiCl}(\text{IPr})(\mu\text{-}\kappa^1\text{-C}\text{:}\kappa^1\text{-N-3-pyridyl})_3]$  complex (in 82% isolated yield). Unlike the 2-pyridyl complexes, this species was catalytically inactive; it was noted that the reactions of 3-chloropyridine catalysed by  $[\text{Ni}(\text{IPr})(\eta^2\text{-styrene})_2]$  also failed to produce the desired product.

The mechanistic landscape for the reactions of  $[\text{Ni}(\text{NHC})_2]$  complexes with organohalides is determined by the structure of the NHC ligand, with small and large NHC ligands often leading to quite different reactivity for the corresponding nickel(0) complex. The reactions between organohalides and  $[\text{Ni}(\text{IMe}^{\text{Me}})_2]$  complexes lead to well-defined *trans*- $[\text{Ni}(\text{R})(\text{X})(\text{IMe}^{\text{Me}})_2]$  complexes (Scheme 16(a)); however,  $[\text{Ni}(\text{Me})(\text{I})(\text{IMe}^{\text{Me}})_2]$  decomposes rapidly once formed ( $\text{IMe}^{\text{Me}} = 1,3,4,5\text{-tetramethylimidazol-2-ylidene}$ ).<sup>80</sup>

Similar, well-behaved two electron behaviour is observed in reactions between  $[\text{Ni}(\text{IiPr})_2(\mu\text{-}\eta^2\text{:}\eta^2\text{-COD})]$  and aryl

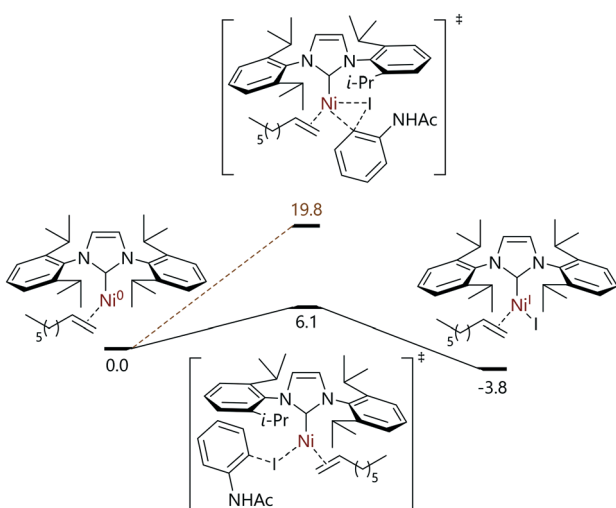
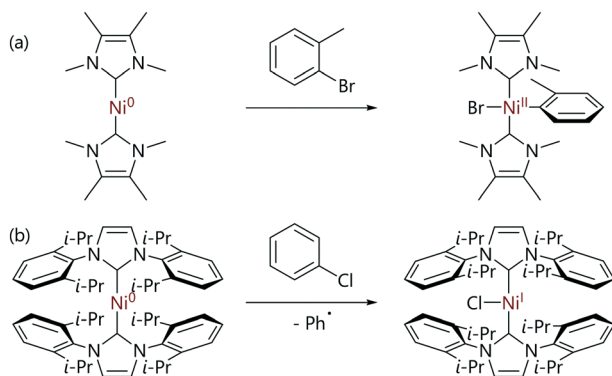


Fig. 4 Halide abstraction as the first step in a tandem photocatalysis/cross-coupling reaction mechanism in which four oxidation states of nickel are invoked.<sup>78</sup>





**Scheme 16** (a) An example of the oxidative addition of aryl halides to a  $[\text{Ni}(\text{NHC})_2]$  complex with a small NHC ligand.<sup>80</sup> (b) An example of the reaction of an aryl halide with an  $[\text{Ni}(\text{NHC})_2]$  complex with a relatively large NHC ligand.<sup>81</sup>

halides, which form  $[\text{Ni}(\text{Ar})(\text{X})(\text{LiPr})_2]$  ( $\text{LiPr} = 1,3\text{-di(iso-propyl)imidazol-2-ylidene}$ ).<sup>83,84</sup> Reactions with aryl halides led to the corresponding acylnickel(II) halide species.<sup>85</sup>

In contrast, the reactions of aryl halides with  $[\text{Ni}(\text{NHC})_2]$  complexes with larger NHC ligands such as IMes and IPr lead to nickel(I) complexes of the form  $[\text{NiX}(\text{NHC})_2]$  (IMes = 1,3-bis(2,4,6-trimethylphenyl)imidazol-2-ylidene) (Scheme 16(b)).<sup>81,86</sup>  $[\text{NiCl}(\text{IPr})_2]$  exists in equilibrium with  $[\text{Ni}(\mu\text{-Cl})(\text{NHC})_2]$  species (often referred to as ‘Sigman’s dimers’)<sup>87</sup> plus free NHC,<sup>81</sup> which can be used to prepare  $[\text{NiCl}(\text{NHC})(\text{PR}_3)]$  complexes by reaction with the corresponding phosphine ligand.<sup>88,89</sup>

Nelson and Maseras investigated this difference in reactivity as a function of NHC size using DFT calculations.<sup>82</sup> The mechanistic proposal that was developed suggested that the difference in reactivity was due to the accessibility of the  $\eta^2$ -complex that precedes oxidative addition. In the case of smaller NHC ligands, the linear C-Ni-C arrangement can bend relatively easily to accommodate an  $\eta^2$ -aryl halide ligand, while for larger NHC ligands such a change in geometry is prohibitively expensive energetically (Fig. 6).

## Summary and outlook

The reactions of nickel(0) complexes with organohalides proceed *via* a range of different mechanisms, and can lead to nickel(I) and/or nickel(II) products. It is apparent that the precise outcomes and mechanisms are a function of both substrate and ligand structure, as well as the coordination number of the nickel(0) complex.

The reactions of nickel(0) complexes with monodentate phosphines with aryl halides can proceed *via* halide abstraction or oxidative addition, while complexes with bidentate phosphines appear to proceed *via* two-electron chemistry. However, the reactions of alkyl halides clearly involve one electron steps such as halide abstraction, but in some cases this is followed by the recombination of the radical with the nickel(I) complex.

Bipyridine-type ligands have long been known to be redox non-innocent, and this is reflected in the reactions of the corresponding nickel(0) complexes. The evidence so far suggests an important role in catalysis for nickel(I) complexes with these ligands, especially in the developing field of tandem photocatalysis/cross-coupling.<sup>90</sup>

The third class of complex that has been examined in this review is NHC-nickel(0) complexes. The reactions of  $[\text{Ni}(\text{NHC})(\text{L})_n]$  complexes can proceed *via* one or two-electron processes, but the factors that determine the pathway of choice in a given reaction remain relatively poorly understood. The situation for  $[\text{Ni}(\text{NHC})_2]$  complexes is rather more well established, with computational evidence suggesting that the size of the NHC ligands in such complexes influences how favourable oxidative addition is *versus* halide abstraction, with the latter requiring far less perturbation of the  $[\text{Ni}(\text{NHC})_2]$  complex from a linear coordination geometry.

There remain a number of practical and conceptual challenges in understanding the reactions of nickel(0) with organochlorides, organobromides, and organoiodides, and some of these are described here:

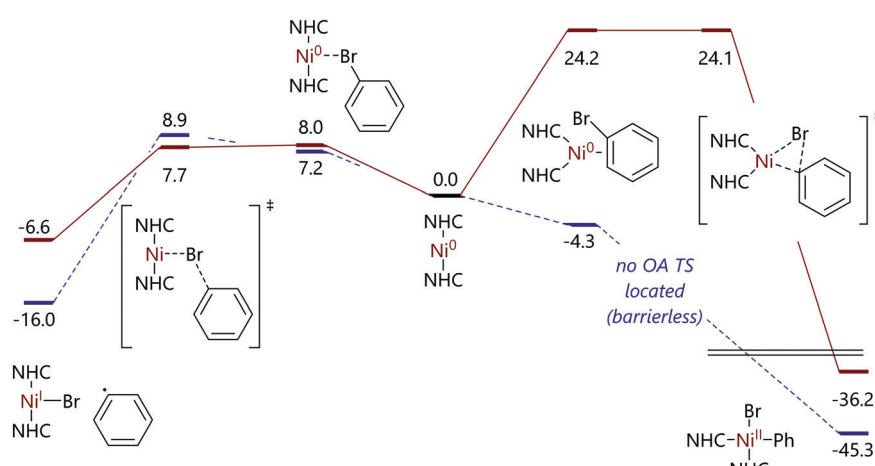


**Fig. 6** Free energy profiles for the reactions of bromobenzene with  $[\text{Ni}(\text{IME}^{\text{Me}})_2]$  and  $[\text{Ni}(\text{IMes})_2]$ .<sup>82</sup>



- Much of our understanding is still based on stoichiometric experiments, which can tell us what is feasible but tells us relatively little about rates; the collection of robust kinetic data for these reactions can be key to understanding the mechanistic features and, importantly, for distinguishing between possible pathways.

- Gathering data, and especially gathering kinetic data, for these systems requires a model complex that is both sufficiently stable to obtain in pure form yet sufficiently reactive to be representative of a process occurring during a catalytic reaction. We have conducted a number of (as yet unpublished) preliminary studies where we have struggled to either isolate the pure nickel(0) complex, where the necessary ancillary ligands make the complex poorly reactive; or where the model complex is insufficiently soluble for a robust kinetic study.

- On a related note, we would urge caution in interpreting ligand comparisons that rely on the formation of an active ligand-nickel complex *in situ*. The combination of a ligand and  $[\text{Ni}(\text{COD})_2]$  does not guarantee the formation of a single well-defined species.<sup>91</sup>

- The role of nickel(i) in catalysis is somewhat behind the scope of this review, although recent work in the area is producing convincing evidence that nickel(i) complexes can mediate some reactions.<sup>62,63,91–93</sup> However, the involvement of nickel(i) *versus* nickel(0) can be difficult to infer, and the mechanism(s) by which a nickel(i) active species might form in a given reaction are often unclear.

- Identifying the products of reactions can be challenging; these could be paramagnetic nickel(i) complexes or paramagnetic or diamagnetic nickel(ii) complexes, for example. While nickel(0) and square planar nickel(ii) complexes lend themselves to analysis using techniques such as NMR spectroscopy, nickel(i) species are often best studied using EPR spectroscopy, and tetrahedral nickel(ii) species are challenging to characterise by either of these methods. This is further complicated by the potential onwards reactions of nickel(i) or nickel(ii) complexes.

- Some substrate classes are less well-studied and are consequently less well understood. The reactions of aryl halides have been explored relatively widely, while alkyl halides are of significant recent interest for us and other researchers. The reactions of vinyl halides with nickel(0) seem to be poorly explored, despite the potential for interesting coordination effects.<sup>38,39,47</sup>

- The reactions of nickel(0) complexes with phosphine ligands form the bulk of the literature in this area, with fewer studies of systems with NHC, bipyridine-type, or mixed (C, N/C, P/N, P) systems. This is likely linked to the challenges in studying these systems using spectroscopic tools, while  $^{31}\text{P}$  NMR spectroscopy is a very convenient tool for monitoring phosphine systems. The redox non-innocent<sup>94</sup> nature of polypyridyl ligand scaffolds provides further challenges; the dimeric, paramagnetic, EPR-silent(!) nickel(i) complex isolated by Hazari's team<sup>9</sup> serves as an example of a system that must have led to significant confusion before a crystal structure was obtained.

Despite these many challenges, this area remains an area of active investigation for us, providing a number of opportunities for academic studies that can lead to useful and impactful applications in catalysis.

The mechanistic complexity of nickel catalysis can in some cases be viewed as a somewhat negative aspect of this field; however, the diversity of reaction pathways that are available will undoubtedly support and underpin the development of new catalytic methodology.

## Author contributions

MEG: investigation, writing – original draft; ELBJH: investigation, writing – original draft; DJN: investigation, supervision, funding acquisition, writing – original draft, writing – review & editing.

## Conflicts of interest

There are no conflicts to declare.

## Acknowledgements

MEG thanks AstraZeneca and the EPSRC for an Industrial CASE Studentship (EP/R512114/1). ELBJH thanks the University of Strathclyde for a Research Excellence Studentship. DJN thanks the University of Strathclyde for a Chancellor's Fellowship (2014–2018). We are grateful to all co-workers, collaborators, and funders – past and present – for their contributions to our research programme in nickel catalysis.

## Notes and references

- 1 S. Z. Tasker, E. A. Standley and T. F. Jamison, *Nature*, 2014, **509**, 299–309.
- 2 J. C. Tellis, C. B. Kelly, D. N. Primer, M. Jouffroy, N. R. Patel and G. A. Molander, *Acc. Chem. Res.*, 2016, **49**, 1429–1439.
- 3 M. H. Shaw, J. Twilton and D. W. C. MacMillan, *J. Org. Chem.*, 2016, **81**, 6898–6926.
- 4 D. J. Weix, *Acc. Chem. Res.*, 2015, **48**, 1767–1775.
- 5 V. P. Ananikov, *ACS Catal.*, 2015, **5**, 1964–1971.
- 6 J. A. Labinger, *Organometallics*, 2015, **34**, 4784–4795.
- 7 M. Portnoy and D. Milstein, *Organometallics*, 1993, **12**, 1665–1673.
- 8 M. M. Roessler and E. Salvadori, *Chem. Soc. Rev.*, 2018, **47**, 2534–2553.
- 9 M. Mohadjer Beromi, G. W. Brudvig, N. Hazari, H. M. C. Lant and B. Q. Mercado, *Angew. Chem., Int. Ed.*, 2019, **58**, 6094–6098.
- 10 C. Hansch, A. Leo and R. W. Taft, *Chem. Rev.*, 1991, **91**, 165–195.
- 11 J. N. Harvey, F. Himo, F. Maseras and L. Perrin, *ACS Catal.*, 2019, **9**, 6803–6813.
- 12 P. Morgante and R. Peverati, *Int. J. Quantum Chem.*, 2020, **120**, e26332.
- 13 T. Sperger, I. A. Sanhueza, I. Kalvet and F. Schoenebeck, *Chem. Rev.*, 2015, **115**, 9532–9586.



14 N. Fey, B. M. Ridgway, J. Jover, C. L. McMullin and J. N. Harvey, *Dalton Trans.*, 2011, **40**, 11184–11191.

15 B. M. Rosen, K. W. Quasdorf, D. A. Wilson, N. Zhang, A.-M. Resmerita, N. K. Garg and V. Percec, *Chem. Rev.*, 2010, **111**, 1346–1416.

16 A. Arévalo and J. J. García, *Eur. J. Inorg. Chem.*, 2010, **2010**, 4063–4074.

17 P. M. Pérez-García and M.-E. Moret, *Chimia*, 2020, **74**, 495–498.

18 D. R. Fahey, *J. Am. Chem. Soc.*, 1970, **92**, 402–404.

19 M. Foa and L. Cassar, *J. Chem. Soc., Dalton Trans.*, 1975, 2572–2576.

20 C. A. Tolman, W. C. Seidel and L. W. Gosser, *J. Am. Chem. Soc.*, 1974, **96**, 53–60.

21 T. T. Tsou and J. K. Kochi, *J. Am. Chem. Soc.*, 1979, **101**, 6319–6332.

22 I. H. Elson, D. G. Morrell and J. K. Kochi, *J. Organomet. Chem.*, 1975, **84**, C7–C10.

23 I. Funes-Ardoiz, D. J. Nelson and F. Maseras, *Chem. – Eur. J.*, 2017, **23**, 16728–16733.

24 A. Manzoor, P. Wienefeld, M. C. Baird and P. H. M. Budzelaar, *Organometallics*, 2017, **36**, 3508–3519.

25 G. Favero, A. Morvillo and A. Turco, *Gazz. Chim. Ital.*, 1979, **109**, 27–28.

26 A. Morvillo and A. Turco, *J. Organomet. Chem.*, 1981, **208**, 103–113.

27 A. L. Clevenger, R. M. Stolley, N. D. Staudaher, N. Al, A. L. Rheingold, R. T. Vanderlinden and J. Louie, *Organometallics*, 2018, **37**, 3259–3268.

28 C. Amatore and A. Jutand, *Organometallics*, 1988, **7**, 2203–2214.

29 L. M. Guard, M. Mohadjer Beromi, G. W. Brudvig, N. Hazari and D. J. Vinyard, *Angew. Chem., Int. Ed.*, 2015, **54**, 13352–13356.

30 M. Mohadjer Beromi, A. Nova, D. Balcells, A. M. Brasacchio, G. W. Brudvig, L. M. Guard, N. Hazari and D. J. Vinyard, *J. Am. Chem. Soc.*, 2017, **139**, 922–936.

31 E. L. Barth, R. M. Davis, M. Mohadjer Beromi, A. G. Walden, D. Balcells, G. W. Brudvig, A. H. Dardir, N. Hazari, H. M. C. Lant, B. Q. Mercado and I. L. Peczak, *Organometallics*, 2019, **38**, 3377–3387.

32 E. Nicolas, A. Ohleier, F. D'Accriscio, A.-F. Pécharman, M. Demange, P. Ribagnac, J. Ballester, C. Gosmini and N. Mézailles, *Chem. – Eur. J.*, 2015, **21**, 7690–7694.

33 C. M. Lavoie, R. McDonald, E. R. Johnson and M. Stradiotto, *Adv. Synth. Catal.*, 2017, **359**, 2972–2980.

34 S. Bajo, G. Laidlaw, A. R. Kennedy, S. Sproules and D. J. Nelson, *Organometallics*, 2017, **36**, 1662–1672.

35 G. Yin, I. Kalvet, U. Englert and F. Schoenebeck, *J. Am. Chem. Soc.*, 2015, **137**, 4164–4172.

36 M. E. Greaves, T. O. Ronson, G. C. Lloyd-Jones, F. Maseras, S. Sproules and D. J. Nelson, *ACS Catal.*, 2020, **10**, 10717–10725.

37 C. Amatore and F. Pfluger, *Organometallics*, 1990, **9**, 2276–2282.

38 A. K. Cooper, D. K. Leonard, S. Bajo, P. M. Burton and D. J. Nelson, *Chem. Sci.*, 2020, **11**, 1905–1911.

39 A. K. Cooper, P. M. Burton and D. J. Nelson, *Synthesis*, 2020, **52**, 565–573.

40 T. T. Tsou, J. C. Huffman and J. K. Kochi, *Inorg. Chem.*, 1979, **18**, 2311–2317.

41 R. Countryman and B. R. Penfold, *J. Cryst. Mol. Struct.*, 1972, **2**, 281–290.

42 A. N. Desnoyer, E. G. Bowes, B. O. Patrick and J. A. Love, *J. Am. Chem. Soc.*, 2015, **137**, 12748–12751.

43 D. J. Mindiola, R. Waterman, D. M. Jenkins and G. L. Hillhouse, *Inorg. Chim. Acta*, 2003, **345**, 299–308.

44 A. N. Desnoyer, W. He, S. Behyan, W. Chiu, J. A. Love and P. Kennepohl, *Chem. – Eur. J.*, 2019, **25**, 5259–5268.

45 W. He and P. Kennepohl, *Faraday Discuss.*, 2019, **220**, 133–143.

46 D. Strawser, A. Karton, O. V. Zenkina, M. A. Iron, L. J. W. Shimon, J. M. L. Martin and M. E. van der Boom, *J. Am. Chem. Soc.*, 2005, **127**, 9322–9323.

47 O. V. Zenkina, A. Karton, D. Freeman, L. J. W. Shimon, J. M. L. Martin and M. E. van der Boom, *Inorg. Chem.*, 2008, **47**, 5114–5121.

48 O. V. Zenkina, O. Gidron, L. J. W. Shimon, M. A. Iron and M. E. van der Boom, *Chem. – Eur. J.*, 2015, **21**, 16113–16125.

49 M. Orbach, S. Shankar, O. V. Zenkina, P. Milko, Y. Diskin-Posner and M. E. van der Boom, *Organometallics*, 2015, **34**, 1098–1106.

50 N. Yoshikai, H. Matsuda and E. Nakamura, *J. Am. Chem. Soc.*, 2008, **130**, 15258–15259.

51 J. A. Bilbrey, A. N. Bootsma, M. A. Bartlett, J. Locklin, S. E. Wheeler and W. D. Allen, *J. Chem. Theory Comput.*, 2017, **13**, 1706–1711.

52 J. Cornellà, C. Zarate and R. Martin, *Chem. Soc. Rev.*, 2014, **43**, 8081–8097.

53 E. D. Entz, J. E. A. Russell, L. V. Hooker and S. R. Neufeldt, *J. Am. Chem. Soc.*, 2020, **142**, 15454–15463.

54 E. Jacobs and S. T. Keaveney, *ChemCatChem*, 2021, **13**, 637–645.

55 C. A. Malapit, J. R. Bour, C. E. Brigham and M. S. Sanford, *Nature*, 2018, **563**, 100–104.

56 P. M. Pérez-García, A. Darù, A. R. Scheerder, M. Lutz, J. N. Harvey and M.-E. Moret, *Organometallics*, 2020, **39**, 1139–1144.

57 D. R. Fahey and J. E. Mahan, *J. Am. Chem. Soc.*, 1977, **99**, 2501–2508.

58 J. K. Stille and A. B. Cowell, *J. Organomet. Chem.*, 1977, **124**, 253–261.

59 A. Zhang, C. Wang, X. Lai, X. Zhai, M. Pang, C.-H. Tung and W. Wang, *Dalton Trans.*, 2018, **47**, 15757–15764.

60 R. Kehoe, M. Mahadevan, A. Manzoor, G. McMurray, P. Wienefeld, M. C. Baird and P. H. M. Budzelaar, *Organometallics*, 2018, **37**, 2450–2467.

61 C. Y. Lin and P. P. Power, *Chem. Soc. Rev.*, 2017, **46**, 5347–5399.

62 I. Kalvet, Q. Guo, G. J. Tizzard and F. Schoenebeck, *ACS Catal.*, 2017, **7**, 2126–2132.



63 J. Jover, *Catal. Sci. Technol.*, 2019, **9**, 5962–5970.

64 G. D. Jones, J. L. Martin, C. McFarland, O. R. Allen, R. E. Hall, A. D. Haley, R. J. Brandon, T. Konovalova, P. J. Desrochers, P. Pulay and D. A. Vicić, *J. Am. Chem. Soc.*, 2006, **128**, 13175–13183.

65 J. T. Ciszewski, D. Y. Mikhaylov, K. V. Holin, M. K. Kadirov, Y. H. Budnikova, O. Sinyashin and D. A. Vicić, *Inorg. Chem.*, 2011, **50**, 8630–8635.

66 B. J. Shields and A. G. Doyle, *J. Am. Chem. Soc.*, 2016, **138**, 12719–12722.

67 S. Biswas and D. J. Weix, *J. Am. Chem. Soc.*, 2013, **135**, 16192–16197.

68 M. Newcomb, in *Encyclopedia of Radicals in Chemistry, Biology and Materials*, 2012, DOI: 10.1002/9781119953678.rad007.

69 The nickel(0) species may be  $[\text{Ni}(\text{COD})(\text{neoc})]$ ,  $[\text{Ni}(\text{neoc})]_2$ , or a mixture of the two, but the ligand was added as 1 molar equivalent with respect to nickelz.

70 A. P. Prakasham and P. Ghosh, *Inorg. Chim. Acta*, 2014, **431**, 61–100.

71 V. Ritleng, M. Henrion and M. J. Chetcuti, *ACS Catal.*, 2016, **6**, 890–906.

72 M. Henrion, V. Ritleng and M. J. Chetcuti, *ACS Catal.*, 2015, **5**, 1283–1302.

73 J. Wu, J. W. Faller, N. Hazari and T. J. Schmeier, *Organometallics*, 2012, **31**, 806–809.

74 Y. Hoshimoto, Y. Hayashi, H. Suzuki, M. Ohashi and S. Ogoshi, *Organometallics*, 2014, **33**, 1276–1282.

75 M. J. Iglesias, J. F. Blandez, M. R. Fructos, A. Prieto, E. Álvarez, T. R. Belderrain and M. C. Nicasio, *Organometallics*, 2012, **31**, 6312–6316.

76 A. J. Nett, S. Cañellas, Y. Higuchi, M. T. Robo, J. M. Kochkodan, M. T. Haynes, J. W. Kampf and J. Montgomery, *ACS Catal.*, 2018, **8**, 6606–6611.

77 S. Felten, S. F. Marshall, A. J. Groom, R. T. Vanderlinden, R. M. Stolley and J. Louie, *Organometallics*, 2018, **37**, 3687–3697.

78 A. de Aguirre, I. Funes-Ardoiz and F. Maseras, *Angew. Chem., Int. Ed.*, 2019, **58**, 3898–3902.

79 S. G. Rull, I. Funes-Ardoiz, C. Maya, F. Maseras, M. R. Fructos, T. R. Belderrain and M. C. Nicasio, *ACS Catal.*, 2018, **8**, 3733–3742.

80 D. S. McGuinness, K. J. Cavell, B. W. Skelton and A. H. White, *Organometallics*, 1999, **18**, 1596–1605.

81 S. Miyazaki, Y. Koga, T. Matsumoto and K. Matsubara, *Chem. Commun.*, 2010, **46**, 1932–1934.

82 D. J. Nelson and F. Maseras, *Chem. Commun.*, 2018, **54**, 10646–10649.

83 T. Zell, M. Feierabend, B. Halfter and U. Radius, *J. Organomet. Chem.*, 2011, **696**, 1380–1387.

84 T. Zell, P. Fischer, D. Schmidt and U. Radius, *Organometallics*, 2012, **31**, 5065–5073.

85 T. Zell and U. Radius, *Z. Anorg. Allg. Chem.*, 2013, **639**, 334–339.

86 K. Zhang, M. Conda-Sheridan, S. R. Cooke and J. Louie, *Organometallics*, 2011, **30**, 2546–2552.

87 B. R. Dible, M. S. Sigman and A. M. Arif, *Inorg. Chem.*, 2005, **44**, 3774–3776.

88 S. Nagao, T. Matsumoto, Y. Koga and K. Matsubara, *Chem. Lett.*, 2011, **40**, 1036–1038.

89 K. Matsubara, Y. Fukahori, T. Inatomi, S. Tazaki, Y. Yamada, Y. Koga, S. Kanegawa and T. Nakamura, *Organometallics*, 2016, **35**, 3281–3287.

90 J. Twilton, P. Zhang, M. H. Shaw, R. W. Evans and D. W. MacMillan, *Nat. Rev. Chem.*, 2017, **1**, 0052.

91 J. Cornella, E. Gómez-Bengoa and R. Martin, *J. Am. Chem. Soc.*, 2013, **135**, 1997–2009.

92 T. Inatomi, Y. Fukahori, Y. Yamada, R. Ishikawa, S. Kanegawa, Y. Koga and K. Matsubara, *Catal. Sci. Technol.*, 2019, **9**, 1784–1793.

93 R. J. Somerville, C. Odena, M. F. Obst, N. Hazari, K. H. Hopmann and R. Martin, *J. Am. Chem. Soc.*, 2020, **142**, 10936–10941.

94 Perhaps we should refer to these systems as 'redox guilty'.

